Electromagnetic Science
vol. 2, no. 3, 0070222, September 2024
https://doi.org/10.23919/emsci.2024.0022

Research Article

On the Directivity of Radiating Quantum Electromagnetic Systems

Said Mikki[1,2]

1. *Zhejiang University-University of Illinois at Urbana-Champaign (ZJU-UIUC) Institute, Zhejiang University, Haining 314400, China*
2. *Department of Electrical and Computer Engineering, University of Illinois at Urbana-Champaign, Urbana 61801-3028, IL, USA*

Corresponding author: Said Mikki, Email: smikki@illinois.edu.
Received April 22, 2024; Accepted July 18, 2024; Published Online August 7, 2024.
Copyright © 2024 The Author(s). This is a gold open access article under a Creative Commons Attribution License (CC BY 4.0).

Abstract — We explore the spatial directivity of radiating quantum source systems, which are defined as any generic source capable of producing photon emission and directing it to specific regions in space. We present a comprehensive definition of quantum directivity, inspired by both classical antenna theory and photon detection theory. Through an in-depth conceptual and mathematical analysis, we identify and address several critical challenges associated with characterizing the directive properties of a general quantum source system. Our approach essentially presents a computational model that relies solely on the density operator of the radiation field as input.

Keywords — Quantum source systems, Directivity, Quantum antennas, Quantum technologies.
Citation — Said Mikki, "On the directivity of radiating quantum electromagnetic systems," *Electromagnetic Science*, vol. 2, no. 3, article no. 0070222, 2024. doi: 10.23919/emsci.2024.0022.

I. Introduction

In recent years, there has been a growing interest in combining electromagnetics with quantum physics for applications in quantum engineering, numerical methods, mathematical physics, and other multidisciplinary fields. A notable example is the emerging field of quantum electromagnetics [1]–[7], which emphasizes the integration of concepts from electromagnetic engineering and theory [8], [9] with quantum mechanics and quantum field theory [10]–[12]. Within this domain, antenna theory, a fundamental area of electromagnetics [13], [14], has prompted interest in developing a unified theory that incorporates both quantum physics and quantum antennas. The main objects studied in this emerging discipline, quantum source systems (QSSs), are conceptualized as directive radiating systems within the framework of quantum antenna theory.

Directive QSSs, most notably quantum antennas but also including quantum sensors [15]–[23], are important elements of quantum information processing systems and are currently investigated for numerous applications ranging from sensing and tomography to nanoelectronics, quantum plasmonics, and quantum information transmission and reception. Quantum antennas are devices designed to emit, receive, and manipulate electromagnetic radiation at the quantum level. Unlike classical antennas, which operate within the regime of classical electromagnetism, quantum antennas are in principle capable of leveraging quantum mechanical properties such as superposition, entanglement, and coherence to enhance their functionality and performance. These antennas are often composed of quantum dots, atomic ensembles, or other nanoscale systems that exhibit quantized energy levels and can interact with single photons or other quantum particles [24]–[29].

Quantum antennas find applications across various cutting-edge fields. In quantum optics, they are used to enhance the efficiency of light-matter interactions, crucial for developing advanced photonic devices [30]. In quantum information processing, quantum antennas play a pivotal role in quantum communication networks, enabling the transmission of quantum states over long distances with minimal loss [23], [31], [32]. They are also instrumental in quantum sensing and metrology, where they enhance the sensitivity and resolution of measurements beyond classical limits [16]. Additionally, quantum antennas are projected to be essential in the development of quantum radar and quantum imaging systems, offering superior resolution and

stealth capabilities [22]. For references covering several of these applications, see for example [22], [33]–[44].

The need for quantum antennas arises from the limitations of classical antennas in handling quantum information and achieving the required precision and control at the nanoscale. Quantum antennas can manipulate quantum states with high fidelity, enabling the realization of quantum networks and the integration of quantum systems into classical infrastructure. They allow for the precise control of photon emission and absorption, which is vital for the development of scalable quantum technologies. Moreover, quantum antennas are expected to operate in regimes where classical antennas are ineffective, such as in the detection of weak signals or in environments with high quantum noise.

A quantum photonic system can focus electromagnetic radiation into specific directions while suppressing it along others through various techniques [45]–[50]. One common method involves using photonic crystals or metamaterials with engineered band gaps and anisotropic properties to direct photons preferentially [51]–[54]. Another approach is the use of quantum interference effects [43], such as those observed in superconducting qubits or cavity quantum electrodynamics systems [55], where constructive and destructive interference can control the spatial distribution of emitted radiation [23]. Additionally, quantum entanglement and coherence can be exploited to synchronize the emission from multiple quantum emitters, achieving directional radiation patterns and enhancing the efficiency of energy transfer [26], [43], [56], [57]. Moreover, resonant cavities, nanoparticles, and waveguides have been shown to be able to control the radiation characteristics of quantum emitters [26], [44], [52], [58]–[60].

The process of the classification of quantum source systems into directive and non-directive ones is crucial for optimizing their application and performance. Directive quantum sources are designed to emit or receive radiation in specific directions, enhancing the signal-to-noise ratio and spatial resolution in applications such as quantum communication, imaging, and sensing [45]–[49], [61]. These sources often employ phased arrays or engineered emission patterns to achieve their directional characteristics [23], [43], [50]. Non-directive quantum sources, on the other hand, emit or receive radiation isotropically or with minimal directional preference, which can be beneficial in applications requiring uniform coverage or omnidirectional sensing. Understanding the distinction between these types of quantum sources aids in the design and implementation of quantum systems tailored to specific applications. For instance, directive sources are preferable in long-distance quantum communication to minimize loss and decoherence, whereas non-directive sources might be better suited for environmental monitoring or distributed quantum networks where uniform detection is desired [34], [43], [47], [61].

The study and development of quantum antennas sit at the intersection of multiple disciplines, including quantum optics, quantum engineering, and quantum information processing. This multidisciplinary nature drives innovation, as insights and techniques from one field can often be adapted and applied to another, leading to breakthroughs that might not be possible within a single discipline [34], [62]. As research in quantum technologies progresses, quantum antennas are expected to play a central role in realizing practical quantum devices and systems, heralding a new era of technological advancement [16], [22], [23].

As mentioned above, since for information transmission a quantum source system is expected to be able to direct energy, i.e., radiated particles in this case, toward specific directions, while suppressing transmission (and sometimes reception) along other directions, and remembering that energy in the quantum domain is proportional to the number of particles [11], [63], then a natural strategy for estimating the directive properties of source systems is to rely on photon statistics [38], [43]. Another strategy is to treat the QSS as an open dynamical system [50], [55], [58], then compute the directivity using accurate stochastic dynamic method such as the GKSL master equation [64] popular in quantum dynamics and information theory [65]–[68]. This strategy is best suited for situations where noise and interference are essential as in quantum communications and quantum information processing in general [69], [70].

The key objective of this article is to formalize a general definition of the directivity of a radiating quantum source system and to provide a thorough conceptual and mathematical foundations for this topic accessible to a wide audience, especially engineers and quantum technologists interested in problems of quantum communication and sensing. Another objective of this article is to show how the proposed directivity can be used to understand and solve the problem of maximizing directivity. Since quantum antennas and sensors are envisioned to send or receive quantum information at different directions, it is imperative to examine how this capacity can be fine tuned by controlling relevant parameters in the radiating configuration such that directivity can become optimum. Optimization of quantum antenna directivity is inherently more complex in the quantum case due to the intrinsically more complex problem of quantum multimode radiation compared with its classical counterpart. Therefore, the purpose of this paper is to provide a clear and rigorous foundations for the topic that can be utilized as a stepping stone toward future applications in communications and sensing.

First, few words about the model itself. We are intentionally avoiding using the term “quantum current” instead of “quantum source” in order to keep the nature of how the system is excited or prepared as flexible as possible. In particular, it is not necessary that the quantum source is a (quantized) current comprised of moving electrons (or other charged particles or molecules). A quantum source might be such a current, but also it can be some externally-controlled potential, an external laser or microwave electromagnetic field, a heat pump, or something completely different based on other physical phenomena. The only impor-

tant formal requirements that a source function in a QSS must satisfy are that it is an externally-controlled structure (so information can be injected for transmission through radiation) and capable of modifying or effecting the directive properties of the emitted quantum radiation [63]. For instance, in classical antenna theory, the directivity of the antenna is a functional of the radiating current source (surface or volume current distributions) [9], [14], [71].

A key issue in defining the directivity of QSS is whether this should be done in space-time or momentum space. Since calculations in quantum theory are considerably easier in momentum space, the latter approach was advocated in some recent approaches [34], [50], [72]–[76], while space-time measures were propounded in few other studies [16], [36], [38], [43]. Both spatio-temporal approaches (using the Feynman propagator method) and momentum space were proposed in [36] within the context of relativistic quantum field theory. However, the main examples considered there (neutral Klein-Gordon field theory) involved massive particles with spin 0. It is therefore of interest to reexamine theoretically this topic from the viewpoint of nonrelativistic quantum electrodynamics, where the main radiation consists of massless bosons (with spin 1), i.e., photons [77]. Certainly, it is the latter scenario that will engage our attention in the subsequent discussion. To streamline matters, in this paper we adopt a non-relativistic framework, eschewing the use of a manifestly covariant formalism. Instead, in what follows we employ the conventional Coulomb gauge second quantization, a customary approach within contemporary quantum optics research [63], [78]–[81].

One of the fundamental conceptual challenges concerning the directivity of electromagnetic source systems, whether they operate in the microwave or optical domain, revolves around the concept of photon *localizability* in space [78]. In essence, this refers to the well-documented issue of the inadequate definitions of photon position or spatial density operators [82]–[84]. This topic is intertwined with the preceding question of whether to define directivity in momentum space or position space. This duality arises due to the Heisenberg uncertainty principle, resulting in the two depictions of the radiating quantum system's directional characteristics being inherently complementary [10], [85]. In the forthcoming discussion, we will explore the proposed position-space directivity formula of a QSS, presented in the context of photon detection theory [80], and demonstrate its nonlocal nature by undertaking a methodical examination employing a rigorous mathematical framework for nonlocality in general QSSs. To analyze nonlocality, we derive the commutator of measurements executed at spatially distant points. This commutator serves as a pivotal tool to quantitatively assess the extent of nonlocality inherent in QSSs. We contend that this nonlocality stands as an essential—perhaps inescapable—attribute across all photonic QSSs. Despite this nonlocality, a certain continuity persists in a manner reminiscent of the parallels observed in the structure of our suggested directivity formula and the directivity of classical antenna systems.

The organizational structure of this paper is outlined as follows. In Section II, we articulate the formulation of quantum directivity in position space and explore the challenge of nonlocality. The distinction between momentum space and space-time formulations is also reviewed. We introduce the proposed directivity formula and meticulously expound on the technical requirements expected from such a quantity, including the careful definition of locality. The justification for the proposed directivity formula is established by drawing an analogy with classical antenna theory and making comparisons with Glauber's photon detection theory. In Section III, we address the related but distinct concept of localizability. Here, we rigorously show that the quantum source system's directivity is nonlocalizable, presenting several exact theorems. These theorems offer quantitative estimates of the deviation from localizability, providing insights into the design of future quantum communication and sensor systems. Section IV engages in detailed discussions and examples to illuminate the main content of our theory. Finally, a series of concluding remarks are presented. Supporting the narrative of the main text, a set of appendices is provided. Appendix A offers a concise summary of the primary field quantization theory, serving as a reference for the theoretical framework deployed in this article. In Appendix B, we present an overview of photon detection theory, a pivotal component underpinning our approach to quantum directivity. Additionally, in Appendix C, we review Mandel's detection operator and compare its directivity with the one proposed in this paper.

II. Directivity Formula in Space and Time

The quantum source system is assumed to produce a quantum radiation field emitted into the surrounding space. The radiation field is expanded into a Fourier sum of creation and annihilation operators as usual in quantum optics and quantum field theory [11], [77], [78], [86], [87]. The specific quantization formalism used in this paper, along with other relevant expressions that will be employed later, is summarized in Appendix A. We have applied the periodic boundary conditions in free space, resulting in the box quantization scheme. This means that our directivity and radiation field phenomena occur in an isotropic and homogeneous vacuum, without any dielectric objects present. In the case of inhomogeneous space or the presence of dielectric objects, one would need to use the electromagnetic Green's functions of dielectric media, significantly complicating the analysis. Instead, this paper focuses on the most fundamental scenario of directive quantum radiation directivity, which occurs in vacuum or free space.

1. Preliminary consideration: momentum space vs. position space

There are two fundamental, yet complementary, modes of viewing the directivity of any radiating system. One can

either view radiation as a process occurring in space-time (position space) or as a process occurring in wavenumber-frequency space. In the first approach, the directive properties of the radiation field are described in terms of the distance r, and the angles θ and φ, measured with respect to the origin of the spatial coordinate frame. In the second approach, the space-time Fourier transform domain (spectral domain) is used to describe the direction in which radiation is directed. These descriptions are complementary due to the fundamental uncertainty relation obeyed by all Fourier transform conjugate pairs [88]. There is an additional complication in the quantum case due to the fact that momentum is proportional to the wavevector $\boldsymbol{k}$, which will be discussed further below.

The fundamental distinctions between considering quantum directivity in either frequency-momentum space or space-time are depicted in Figure 1. A quantum source is defined as a space-time function $\boldsymbol{J}_{\rm s}(\boldsymbol{x},t)$ that externally controls the directive properties of the quantized radiation field [36]. Here, the source function has a compact support on $D_{\rm s} \subset \mathbb{R}^4$. The spherical coordinate system is $\boldsymbol{x} = [r\ \ \theta_{\boldsymbol{x}}\ \ \varphi_{\boldsymbol{x}}]^{\rm T}$, where T is the transpose operation, while $\theta_{\boldsymbol{x}}$ and $\varphi_{\boldsymbol{x}}$ are spherical angles associated with $\boldsymbol{x}$. In Fourier space, also known as momentum space, we work with the Fourier transform of the source function, denoted as $\boldsymbol{J}_{\rm s}(\boldsymbol{k},\omega)$, where $\boldsymbol{k} \in \mathbb{R}^3$ is the wavevector and $\omega \in \mathbb{R}^+$ is the radian frequency. The field quantization procedure (Appendix A) is formulated in this momentum space representation. When examining the directivity within this framework, the direction along which a photon propagates can be analyzed by considering the strength of photon motion along the direction specified by the unit vector $\hat{k}(\Omega_{\boldsymbol{k}}) := \boldsymbol{k}/|\boldsymbol{k}|$, where $\Omega_{\boldsymbol{k}} = (\theta_{\boldsymbol{k}}, \varphi_{\boldsymbol{k}})$ represents the solid angle with $\theta_{\boldsymbol{k}}$ and $\varphi_{\boldsymbol{k}}$ being the spherical angles associated with $\boldsymbol{k}$. As illustrated in Figure 1(a), a rotating momentum or $\boldsymbol{k}$-space point exhibits a changing direction defined by the solid angle $\Omega_{\boldsymbol{k}}$ with a magnitude of $|\boldsymbol{k}| = \omega/c$, where c is the speed of light. Therefore, within the momentum space approach, meaningful questions can be posed regarding the direction of the momentum/wavevector $\boldsymbol{k}$. However, as will be discussed below, within the momentum space formalism, the radial distance becomes indeterminate.

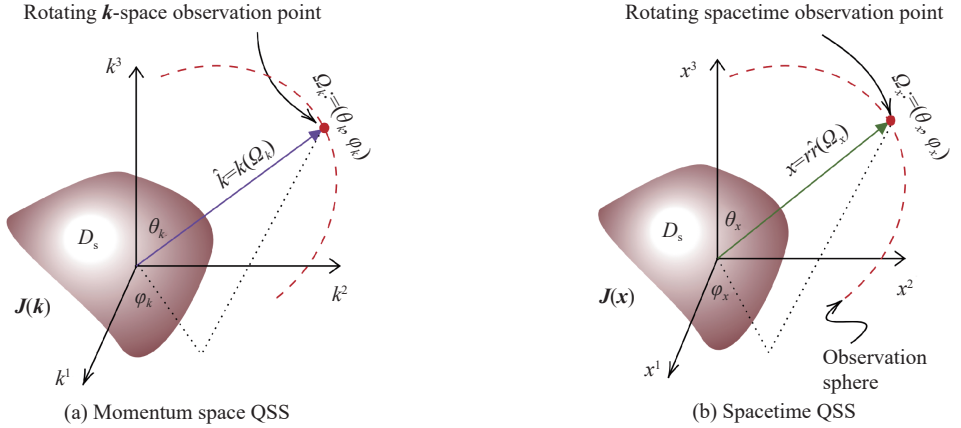


Figure 1 Mathematical representation of the directivity space in quantum source systems (QSSs). (a) Momentum space; (b) Space-time.

The momentum space approach facilitates more direct and streamlined calculations, benefiting from the advantageous formulation of quantum field theory in Fourier or $\boldsymbol{k}$-space representation [34], [50], [72]–[76]. However, within this framework, precise information about the exact photon positions cannot be obtained due to the inherent uncertainty relation of the Fourier transform [85]. Consequently, both classical [89] and quantum scenarios [36] suffer from the limitation of the lack of exact spatial localization of electromagnetic radiation. In practical terms, when seeking to assess the energy (number of emitted photons) guided by a given QSS along a specific spatial direction defined by spherical angles $\theta_{\boldsymbol{k}}$ and $\varphi_{\boldsymbol{k}}$, as shown in Figure 1(a), i.e., in momentum space, the resulting estimation becomes undetermined with respect to the radial distance r or range from the QSS itself. Consequently, information regarding whether the directed energy predominantly falls within the deep near-field (NF) zone, intermediate NF zone, or far-field zone remains elusive.

To obtain the missing position-space information, the alternative—in fact complementary—approach of position space directivity is naturally proposed, aiming to assess the intensity of emitted radiation at specific spatial locations. Figure 1(b) illustrates the fundamental structure of this description. Unlike Figure 1(a), where the spherical angles are associated with the direction of momentum or wave vector $\boldsymbol{k}$, in this case, they are instead correlated with the position vector $\boldsymbol{x}$. A rotating point in $\boldsymbol{x}$-space can provide information about the direction in which photons would flow, specified by the angle $\Omega_{\boldsymbol{x}}$. Additionally, the radial distance $r = |\boldsymbol{x}|$ can also be determined. Consequently, insights into the intensity of quantum radiation can be derived at any spatial position, encompassing both near-field and far-field zones. However, it should be noted that the meaning of the direction vector $\hat{r} = (\theta_{\boldsymbol{x}}, \varphi_{\boldsymbol{x}})$ in position space is no longer intuitively associated with momentum, as depicted in Figure 1(a).

In momentum space, the "strength" of the photon's motion in a given direction can be directly related to the magnitude of the momentum in that direction. In contrast, in position space, this intuitive picture is no longer applicable, as the direction of $\boldsymbol{x}$ does not convey a direct physical representation of the "strength" of the photon motion along that direction. Therefore, in this paper, we propose interpreting position-space directivity in terms of the (measurable) photon's detector counting rates rather than the "intrinsic" momentum or energy of the photon itself.

The spacetime formulation introduced in [36] employed the concept of probability amplitude and Feynman propagators to directly assess the intensity of quantum radiation at specific points in spacetime, regardless of whether they are near or far from the source domain. Notably, this formulation demonstrated the convenient property of Lorentz covariance. In the subsequent discussion, we present an alternative approach that characterizes the directivity of the QSS by considering the averaged values of distinct quantum operators, which are readily measurable. Moreover, we present this tailored formulation specifically for photons, as opposed to the massive Klein-Gordon particles that were the central focus of the aforementioned study. Additionally, to enhance accessibility, we refrain from demonstrating manifest Lorentz covariance, as we utilize the widely-used Coulomb-gauge formulation.

2. Problem of photon nonlocalizability in position space

A significant technical challenge arises when transitioning from the momentum space to the position space approach for analyzing directivity, particularly in the case of photons. This challenge stems from the inherent non-localizability of photons in position space. To grasp the essence of this issue, consider the scenario in momentum space where we aim to establish a spatial direction representation based on the $\boldsymbol{k}$ vector direction. Since the momentum operator $\boldsymbol{p} = \hbar \boldsymbol{k}$, where $\hbar$ is the reduced Planck constant, is well-defined for photons, this leads to relatively straightforward calculations, as demonstrated in works like [50], [55]. On the contrary, photons lack a well-defined position operator due to the absence of a general wavefunction for them [90]. Notably, a compelling theorem formulated by Newton and Wigner establishes that particles with zero mass cannot possess a well-behaved position operator defined in accordance with natural and reasonable expectations [82].[*1] However, despite the implications of the Newton-Wigner theorem, extensive research spanning the past seven decades has been dedicated to addressing the challenge of photon localization from a foundational perspective.[*2] Despite these efforts, a universally accepted position-space-based photon wave function remains elusive, with proposals for such a formalism periodically emerging. For the context of our current paper, which primarily revolves around devising a practical and straightforward approach for characterizing the directivity of quantum antenna systems, we treat the non-localizability of photons as a foundational attribute that distinguishes quantum antennas from their classical counterparts.

Nevertheless, there exists an alternative avenue for addressing photon localization that avoids the requirement of photon position operators. This approach revolves around seeking suitable operators that exhibit two appealing attributes [86], [100] as follows:

1) The ability to approximate photon localization behavior in space in the sense that the proposed operator provide information about the QSS radiation field in concentrated spatial regions of the surrounding space.

2) The measurability of the proposed operator within laboratory setting.

In Figure 2, we show a scenario where instead of asking about the directivity at a point in space, we attempt instead to estimate how many photons are concentrated in a specific volume in space. Let $V_{\boldsymbol{x}_1}$ and $V_{\boldsymbol{x}_2}$ be two arbitrary regions labeled by the positions $\boldsymbol{x}_1 \in V_{\boldsymbol{x}_1}$ and $\boldsymbol{x}_2 \in V_{\boldsymbol{x}_2}$, respectively. If the volumes of the regions $V_{\boldsymbol{x}_1}$ and $V_{\boldsymbol{x}_2}$ shrinks to zero while keeping $\boldsymbol{x}_1$ and $\boldsymbol{x}_2$ included, then we may consider the number operators associated with these limits as representation of the quantum radiation localization around $\boldsymbol{x}_1$ and $\boldsymbol{x}_2$, and hence make a comparison between the directivities of the QSS at different locations in space.

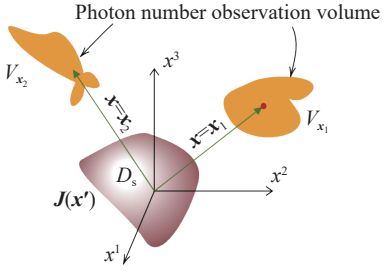


Figure 2 Spatial regions where the density of the photons is to be estimated at multiple positions around the source in order to characterize the directive properties of the QSS. Here, we think of $V_{\boldsymbol{x}}$ as a topological neighborhood of $\boldsymbol{x} \in V \subset \mathbb{R}^3$.

3. Definition of the directivity of a generic quantum source system

In anticipation of the subsequent discussion, we introduce the principal definition of this paper, offering a metric for estimating the angular directivity of a QSS in space-time.

Definition 1 (Quantum antenna directivity in space-time) Consider a QSS with field operator $\boldsymbol{E}(\boldsymbol{x},t) = \boldsymbol{E}^{(+)}(\boldsymbol{x},t) + \boldsymbol{E}^{(-)}(\boldsymbol{x},t)$ and a radiation state density operator ρ. Then the angular directivity at distance $|\boldsymbol{x}|$ from origin is defined as follows:

[*1]Note that this complication did not arise in the relativistic formulation presented in [36], where the calculations pertained to massive Klein-Gordon particles. Particles with non-zero mass can indeed be localized, as a well-defined position operator can be established in such cases.

[*2]Several notable works in this area include [78], [82]–[84], [91]–[97]. A particularly lucid conceptual exploration of the localization problem in quantum field theory can be found in [98]. A recent review (up to 2015) is given in [99].

$$\mathcal{D}_q(|\boldsymbol{x}|,\Omega;t) := \frac{\mathrm{Tr}\{\rho \boldsymbol{E}^{(-)}(\boldsymbol{x},t)\cdot\boldsymbol{E}^{(+)}(\boldsymbol{x},t)\}}{\frac{1}{4\pi}\int_{4\pi}\mathrm{d}\Omega\,\mathrm{Tr}\left\{\rho \boldsymbol{E}^{(-)}(\boldsymbol{x},t)\cdot\boldsymbol{E}^{(+)}(\boldsymbol{x},t)\right\}} \quad (1)$$

whenever the denominator of (1) is not identically zero. If the denominator is zero, then the directivity of the QSS is not defined.

A rigorous justification for this definition is provided in detail below.[*3] In the meantime, let's offer a brief overview illustrating its intuitive rationale. Initially, observe the numerator, denoting the expected value of the operator $\boldsymbol{E}^{(-)}(\boldsymbol{x},t)\cdot\boldsymbol{E}^{(+)}(\boldsymbol{x},t)$. This quantity can be interpreted as the counting rate of a point-like isotropic wideband photon detector positioned at $\boldsymbol{x}$ and generating the measurement at time t. For more information on this interpretation, refer to Appendix B, which examines Glauber's photon detection theory, with the expression (B-11) providing relevant insights.

On the contrary, the denominator in (5), representing the angular average of the quantity from the numerator, demands a more meticulous justification. This is because it presupposes that $\boldsymbol{E}^{(-)}(\boldsymbol{x},t)\cdot\boldsymbol{E}^{(+)}(\boldsymbol{x},t)$ can be construed as a form of photon density operator in space (refer to Figure 2 for an illustration when V_x diminishes to a point $\boldsymbol{x}$). Such an interpretation is not inherently evident and necessitates a thorough and rigorous examination, as expounded in Sections II.4 and II.5 below.

4. Search for a suitable local number operator for quantum source systems

In principle, the general discussion provided in Section II.2 regarding photon nonlocalizability need not be fundamentally connected solely with the photon number operator, as the issue is more general. However, number operators have a long history in quantum field theory, particularly in the search for local density operators capable of localizing the photon's position in space. Moreover, it turns out that the local number operator, as will be shown below, provides the best route for a rigorous and consistent justification of the directivity formula (1). For these reasons, we focus on number operators and their commutators as the main theoretical background for a deeper understanding of the directivity of quantum source systems.

Before we proceed with the discussion, we wish to highlight a potential confusion that may arise between two technical terms employed in this paper: "local operator" and "localizable operator". The distinction stems from the fact that a local photon number operator may or may not be localizable. In other words, being a local operator is different from being localizable. In this paper, we adhere to the following definitions: Local operators, as described earlier, provide insights into the field's behavior within a neighbourhood $V_x \subset \mathbb{R}^3$ (refer to Figure 1 and Definition 2). Conversely, the definition of localizability (as per Definition 3) pertains to the ability to measure the field independently in two non-overlapping spatial regions.

In quantum optics, a prevalent option is to explore operators such as the number operator, with a particular focus on number densities [78]. However, a common issue encountered with such number operators is that, when confined to local regions in space, they do not consistently yield well-defined, i.e., non-negative, expected values. To clarify this issue and provide motivation for the specific definition proposed in this paper, we begin by revisiting how the problem arose in the context of quantum field theory and quantum optics. Recall that the number operator is given by [63]

$$N = \frac{2\varepsilon_0}{\hbar c}\int_{\mathbb{R}^3}\mathrm{d}^3x\,\boldsymbol{E}^{(-)}(\boldsymbol{x})\cdot(-\nabla^2)^{-1/2}\boldsymbol{E}^{(+)}(\boldsymbol{x}) \quad (2)$$

where ε_0 is the electric permittivity of free space and the operator $(-\nabla^2)^{-1/2}$ is defined in Appendix A.

It is essential that the integration is performed over the entire space. In order to construct a local operator, we need to determine suitable number operators associated with a given region V, denoted as $N(V)$. The most straightforward choice is to redefine the integration domain in (2) from $\mathbb{R}^3$ to V [78], [101]. However, due to the non-positive definite integrand in (2), the average of this operator might be negative (it can be shown that when $V = \mathbb{R}^3$, the average of N is always positive.) Various proposals have been made to circumvent this issue by modifying the definition of the local number operator, such as the Mandel operator [78], [102]. Because of its historical importance and to show how our proposed approach differs from it, we review the Mandel operator approach in Appendix C. While we do not employ Mandel's operator $\boldsymbol{M}$ in constructing the QSS's directivity in this paper, it can be beneficial for a broad audience to be acquainted with one of the popular approaches to local operators in quantum optics—the Mandel's operator approach.

As will be demonstrated shortly, the directivity expression (C-3) in Appendix C based on Mandel's approach is considerably more complex to calculate and less straightforward to interpret than the one proposed below. The latter's direct interpretation is the counting rate of the photon detection operator (see Appendix B).

In the subsequent discussion, we introduce a quantum antenna directivity definition based on an alternative approach to local number operators suggested in [100]. However, prior to that, we need to establish a general definition for what we consider an acceptable local operator.

Definition 2 (Local number operators) Consider a subset $V \subset \mathbb{R}^3$. We define a local number operator $N(V)$ as a quantum Hermitian operator with the property that its average value[*4] is always non-negative for any $V \subset \mathbb{R}^3$.

In an intuitive sense, a local number operator func-

[*3] Cf. Section II.5.

[*4] The average value produced by a suitable measurement process is defined as $\mathrm{Tr}\rho N(V)$, where ρ is the quantum state.

tions as an approximation for the count of photons concentrated within a spatial region $V \subset \mathbb{R}^3$, modulo a linear operator. Put differently, the average value of this operator $N(V)$ in the specific quantum state is directly proportional to the anticipated number of measurable photons within the region V (refer to Figure 2 for illustration). This form of localization is crucial to achieve a coherent interpretation of the directivity formula (1). It enables a consistent comparison with the corresponding classical directivity, as explained in Section II.5.

Remark 1 As we have previously observed, the attempt to constrain the total number operator within finite subregions proves ineffective due to its inability to maintain positivity. For completeness, we summarize that notable fact by the following proposition: The operator $N(V)$ defined by

$$N(V) := \frac{2\varepsilon_0}{\hbar c}\int_{x\in V} \mathrm{d}^3x\, \boldsymbol{E}^{(-)}(\boldsymbol{x})\cdot(-\nabla^2)^{-1/2}\boldsymbol{E}^{(+)}(\boldsymbol{x}) \tag{3}$$

is not a local number operator.

Motivated by the approach proposed by Deutsch *et al.* in [100] to deal with quantum beam optics, we propose the following form for the radiating QSS local number operator:

$$N(V) = \frac{2\varepsilon_0}{\hbar c}\int_{x\in V} \mathrm{d}^3x\, \boldsymbol{E}^{(-)}(\boldsymbol{x},t)\cdot\boldsymbol{E}^{(+)}(\boldsymbol{x},t) \tag{4}$$

This definition draws direct inspiration from Glauber's theory of photon detection [80]. To see the rationale behind this choice, refer back to (B-11) and the corresponding discussion in Appendix B, where it is shown that the average of the operator (4) offers an estimation of the counting rate of an isotropic wideband photon detector located within the volume V. The presence of a linear factor in this relation establishes a connection between the average value and the photon number, characterized by $D^{-1}\mathrm{d}/\mathrm{d}t$ (cf. Appendix B). Additionally, it is evident that the integrand within (4) serves as a positive definite operator, ensuring that the average of $N(V)$ remains positive for any $V \subset \mathbb{R}^3$. Consequently, all conditions stipulated in Definition 2 are satisfied, culminating in the following theorem:

Theorem 1 The operator $N(V)$ defined through (4) is a local number operator.

5. Justification and discussion of the proposed definition of the directivity of a quantum source system

Armed by the result that the operator $N(V)$ is local (Theorem 1), let us now proceed forward to employ the local photon detection operator (4) to establish a definition for the directivity of a radiating QSS.

To begin, we will revisit the classical antenna directivity definition. Assume that the radiation intensity of a classical antenna at frequency ω in the far-zone is described as $U_{\mathrm{rad}}(\boldsymbol{x};\omega) = |\boldsymbol{x}|^{-2}U(\Omega;\omega)$. The overall time-harmonic radiated power across all solid angles Ω is given by $P_{\mathrm{rad}}(|\boldsymbol{x}|;\omega) = |\boldsymbol{x}|^{-2}\int_{4\pi}\mathrm{d}\Omega U(\Omega;\omega)$. Within this context, the directivity is defined as follows [13], [14]:

$$\mathcal{D}(\Omega;\omega) := \frac{U(\Omega;\omega)}{P_{\mathrm{rad}}(|\boldsymbol{x}|;\omega)/4\pi} = \frac{U(\Omega;\omega)}{\int_{4\pi}\mathrm{d}\Omega U(\Omega;\omega)/4\pi} \tag{5}$$

It is important to note that in the far-field zone, the directivity becomes an angular function and remains independent of the radial distance $|\boldsymbol{x}|$ from the origin [71]. Physically, the directivity provides a measure of the amount of energy the antenna can effectively radiate along the direction Ω, when compared to the radiation distribution of an ideal isotropic radiator characterized by a constant value of $P_{\mathrm{rad}}/4\pi$ [13].

Moving now to the quantum case, the local number *density* operator corresponding to (4) can be obtained with the help of the formula

$$U^q_{\mathrm{rad}}(\boldsymbol{x},t) := \lim_{\|V\|\to 0}\frac{N(V)}{\|V\|} = \frac{2\varepsilon_0}{\hbar c}\boldsymbol{E}^{(-)}(\boldsymbol{x},t)\cdot\boldsymbol{E}^{(+)}(\boldsymbol{x},t) \tag{6}$$

where $\|V\|$ is the volume of the region V. Inspired by the classical antenna directivity formula (5), we may now define the quantum antenna directivity by (1), Definition 1 above.

Remark 2 The expression $\mathrm{Tr}\{\rho\boldsymbol{E}^{(-)}(\boldsymbol{x},t)\cdot\boldsymbol{E}^{(+)}(\boldsymbol{x},t)\}$ can be evaluated in either the Heisenberg or interaction picture. In the Heisenberg picture, the field operators evolve according to the full Hamiltonian, while the state ρ remains time-independent. On the other hand, in the interaction picture, we evolve $\boldsymbol{E}(\boldsymbol{x},t)$ based on the free Hamiltonian as given by (B-3) in Appendix B, while ρ becomes time-dependent through evolution under the interaction Hamiltonian.

Remark 3 When comparing (5) with (1), it becomes evident that our quantum directivity definition aligns most naturally with the time domain, whereas the classical antenna's definition pertains to the frequency domain. Although not inherently conceptually significant, this disparity underscores certain fundamental structural distinctions between classical and quantum radiation. Nevertheless, if we operate within the Heisenberg picture and apply the unimpeded or free evolution of the field operators as described in (B-3), the contrast between these two expressions loses its significance, given that (B-3) indeed exhibits a structure remarkably akin to the phasor representation found in classical quantities.

The rationale behind Definition 1 stems from the fact that the quantity featured in the numerator of (1) signifies the photon detection rate at the position $\boldsymbol{x}$. Referring to (6), this essentially represents an average of a photon number density operator. Consequently, in order to formulate an ideal reference isotropic radiator at the position $|\boldsymbol{x}|$, we integrate the numerator across all solid angles 4π and then normalize by dividing it by 4π to yield the isotropic radiation density. It is worth noting that the constant factors $2\varepsilon_0/\hbar c$ appearing in (4) mutually cancels out in this process. Additional comments and analysis of this definition can be found below in Sections IV and V. We next turn to the important question of localizability.

If we compare the proposed definition of directivity

above with another possible expression (not derived by Mandel himself but given here for the first time), namely expression (C-3), we immediately notice that due to the existence of the operator $(-\nabla^2)^{1/4}$ in the latter case, the Mandel-based directivity is considerably more complex to evaluate. In addition, our proposed definition, which is based on the different local number operator (4), yields a more straightforward interpretation in terms of the counting rates of photon detectors in Glauber's detection theory (see Appendix B).

III. Nonlocalizablity of the Directivity of Electromagnetic Quantum Systems

We proceed to establish the concept of nonlocalizability for a local number operator, a notion distinct from the nonlocality commonly associated with quantum entanglement. The most natural and commonly employed approach is to establish this property based on the commutativity of nonoverlapping support domains. This methodology is inspired by the fundamental principle in quantum physics—especially quantum field theory—that two experimentally measurable observables are considered independent if they commute [77].

Definition 3 (Nonlocalizablity) Consider a given local operators. Let $V \subset \mathbb{R}^3$ and $V' \subset \mathbb{R}^3$ be two subsets. Then if the following condition holds

$$\exists V, V' \subset \mathbb{R}^3 \mid V \cap V' = \varnothing \implies [N(V), N(V')] \neq 0 \tag{7}$$

we say that $N(V)$ is nonlocalizable. A localizable operator is a local operator that is never nonlocalizable.

Intuitively, the notion of localizability presented here differs from the locality defined in Definition 1. Localizability inherently conveys the natural expectation that measurements conducted in spatially separated regions should be independent. In quantum field theory and quantum optics, independence is captured by commutativity, where Hermitian operators corresponding to independent observables commute [77]. Conversely, if the operators of two observables do not commute, measuring one inevitably influences the other observable. It's important to note the distinction from the concept of locality introduced in Definition 1, where the primary requirement in the latter is that the average value of $N(V)$ reflects the number of photons in a neighborhood of $\boldsymbol{x} \in \mathbb{R}^3$—i.e., that V contains a topological neighborhood for some $x \in V \subset \mathbb{R}^3$.

Considering the widely recognized absence of a position-space wavefunction for photons [90] and the inadequate nature of several proposed alternatives aimed at approximating localizable number density operators[*5], it's reasonable to expect that the quantum antenna directivity construction provided in Definition 1 would similarly result in nonlocal characteristics. As will be demonstrated below, this is indeed the case as the subsequent theorem illustrates.

Theorem 2 The operator (4) is nonlocalizable.

Proof Without loss of generality, we work in the Schrodinger picture and set $2\varepsilon_0/\hbar c = 1$, allowing us to rewrite (4) as

$$N(V) = \int_{\boldsymbol{x}\in V} \mathrm{d}^3 x\, \boldsymbol{E}^{(-)}(\boldsymbol{x}) \cdot \boldsymbol{E}^{(+)}(\boldsymbol{x}) \tag{8}$$

To further simplify the presentation, we deploy the shorthand notation $E_i := E_i^{(+)}(\boldsymbol{x})$, $E_i' := E_i^{(+)}(\boldsymbol{x}')$, where $\boldsymbol{E}^{(+)} = \sum_{i=1}^3 E_i \hat{x}_i$. From the bi-linearity of the commutator, we get

$$[N(V), N(V')] = \int_V \mathrm{d}^3 x \int_{V'} \mathrm{d}^3 x' \sum_{i=1}^3 \sum_{j=1}^3 \left[E_i^\dagger E_i, E_j'^\dagger E_j'\right] \tag{9}$$

Utilizing the standard commutator identity

$$[AB, CD] = A[B, C]D + [A, C]BD + CA[B, D] + C[A, D]B \tag{10}$$

we can evaluate

$$\left[E_i^\dagger E_i, E_j'^\dagger E_j'\right] = E_i^\dagger \left[E_i, E_j'^\dagger\right] E_j' + E_j'^\dagger \left[E_i^\dagger, E_j'\right] E_i \tag{11}$$

where (A-9) was used to nullify the second and third terms in the right-hand side (RHS) of (10). Next, with the help of (A-7), the commutators in the RHS of (11) can be evaluated, leading to

$$\left[E_i^\dagger E_i, E_j'^\dagger E_j'\right] = (E_i^\dagger E_j' - E_j'^\dagger E_i)(-\nabla^2)^{1/2} \delta_{ij}^\perp(\boldsymbol{x} - \boldsymbol{x}') \tag{12}$$

where we have used the fact that $\delta_{ij}^\perp(\boldsymbol{x} - \boldsymbol{x}') = \delta_{ij}^\perp(\boldsymbol{x}' - \boldsymbol{x})$.[*6] Substituting (12) into (9), we arrive at

$$\begin{aligned}&[N(V), N(V')] \\ &= \sum_{ij=1}^3 \int_V \mathrm{d}^3 x \int_{V'} \mathrm{d}^3 x' [(-\nabla^2)^{1/2} \delta_{ij}^\perp(\boldsymbol{x} - \boldsymbol{x}')] \mathcal{E}_{ij}(\boldsymbol{x}, \boldsymbol{x}')\end{aligned} \tag{13}$$

where the operator $\mathcal{E}_{ij}(\boldsymbol{x}, \boldsymbol{x}')$ is defined by

$$\mathcal{E}_{ij}(\boldsymbol{x}, \boldsymbol{x}') := E_i^{(-)}(\boldsymbol{x}) E_j^{(+)}(\boldsymbol{x}') - E_j^{(-)}(\boldsymbol{x}') E_i^{(+)}(\boldsymbol{x}) \tag{14}$$

We will now show that when $V \cap V' = \varnothing$, the commutator $[N(V), N(V')]$ does *not* vanish. First, we note that in quantum field theory the dependence of field operators on space generally comes in the form of linear combinations of the form $\hat{\mathcal{E}}_{ij}\tilde{\mathcal{E}}_{ij}(\boldsymbol{x}, \boldsymbol{x}')$, where $\hat{\mathcal{E}}_{ij}$ is an operator with no spatial dependence and $\tilde{\mathcal{E}}_{ij}(\boldsymbol{x}, \boldsymbol{x}')$ is a complex-valued spatial function [77], [103]. Consequently, we will replace $\mathcal{E}_{ij}(\boldsymbol{x}, \boldsymbol{x}')$ by $\hat{\mathcal{E}}_{ij}\tilde{\mathcal{E}}_{ij}(\boldsymbol{x}, \boldsymbol{x}')$ even though the former is in general a linear combination of terms with the latter's form. For example, it is clear from field expansions such as (A-4) that the operator $\mathcal{E}_{ij}(\boldsymbol{x}, \boldsymbol{x}')$ may be written as a sum of space-independent operators of the form $a^\dagger a$, aa, $a^\dagger a$, and so on, multi-

[*5] Cf. Section II and references cited therein.
[*6] Recall that as in (A-7), the operator $(-\nabla^2)^{1/2}$ is applied to the $\boldsymbol{x}$-function.

plied by exponential functions of the form $\exp[\mathrm{i}\boldsymbol{k}\cdot(\boldsymbol{x}-\boldsymbol{x}')]$, etc. Based on this understanding, using (12), and with a slight abuse of notation, we find the following:

$$\begin{aligned}
&[N(V),N(V')]\\
&\sim \sum_{ij=1}^{3}\int_V \mathrm{d}^3x\int_{V'}\mathrm{d}^3x'\,[(-\nabla^2)^{1/2}\delta_{ij}^{\perp}(\boldsymbol{x}-\boldsymbol{x}')]\hat{\mathcal{E}}_{ij}\tilde{\mathcal{E}}_{ij}(\boldsymbol{x},\boldsymbol{x}')\\
&=\sum_{ij=1}^{3}\hat{\mathcal{E}}_{ij}\int_{V'}\mathrm{d}^3x'\int_V \mathrm{d}^3x\,\tilde{\mathcal{E}}_{ij}(\boldsymbol{x},\boldsymbol{x}')(-\nabla^2)^{1/2}\delta_{ij}^{\perp}(\boldsymbol{x}-\boldsymbol{x}')\\
&=\sum_{ij=1}^{3}\hat{\mathcal{E}}_{ij}\int_{V'}\mathrm{d}^3x'\int_V \mathrm{d}^3x\,\delta_{ij}^{\perp}(\boldsymbol{x}-\boldsymbol{x}')(-\nabla^2)^{1/2}\tilde{\mathcal{E}}_{ij}(\boldsymbol{x},\boldsymbol{x}')\\
&=\sum_{ij=1}^{3}\hat{\mathcal{E}}_{ij}\int_{V'}\mathrm{d}^3x'\int_V \mathrm{d}^3x\,\delta_{ij}^{\perp}(\boldsymbol{x}-\boldsymbol{x}')\tilde{\mathcal{E}}'_{ij}(\boldsymbol{x},\boldsymbol{x}')\\
&=\sum_{ij=1}^{3}\hat{\mathcal{E}}_{ij}\int_{V'}\mathrm{d}^3x'\int_V \mathrm{d}^3x\,\delta_{ij}\delta(\boldsymbol{x}-\boldsymbol{x}')\tilde{\mathcal{E}}'_{ij}(\boldsymbol{x},\boldsymbol{x}')\\
&\quad+\sum_{ij=1}^{3}\hat{\mathcal{E}}'_{ij}\int_{V'}\mathrm{d}^3x'\int_V \mathrm{d}^3x\frac{1}{4\pi}\nabla_i\nabla_j\frac{1}{|\boldsymbol{x}-\boldsymbol{x}'|}\tilde{\mathcal{E}}'_{ij}(\boldsymbol{x},\boldsymbol{x}') \qquad (15)
\end{aligned}$$

where $\tilde{\mathcal{E}}'_{ij}(\boldsymbol{x},\boldsymbol{x}')$ is defined by $\tilde{\mathcal{E}}'_{ij}(\boldsymbol{x},\boldsymbol{x}') := (-\nabla^2)^{1/2}\tilde{\mathcal{E}}_{ij}(\boldsymbol{x},\boldsymbol{x}')$. In the second equality in (15) we interchanged the order of the integrals. The third and last equalities in (15) were derived by applying the integration by parts formula (A-8) to the $\boldsymbol{x}'$-integral and the transverse delta function expansion in space (A-11), respectively.

We finally note that the first term in the last equality in (15) vanishes since by assumption the volumes V and V' are nonoverlapping. On the other hand, the second term containing the second-order derivative $\nabla_i\nabla_j\frac{1}{|\boldsymbol{x}-\boldsymbol{x}'|}$ does not vanish. In fact, it decays slowly, with decay rate of R^{-3}, $R := |\boldsymbol{x}-\boldsymbol{x}'|$, or faster. Therefore, the commutator $[N(V),N(V')]$ does not vanish on some nonzero function $F(\boldsymbol{x})$. □

We can improve on Theorem 2 by providing an explicit calculation of the decay rate of the local field density operator commutators.

Theorem 3 Let $V,V'\subset\mathbb{R}^3$ be disjoint regions in space. Then the commutator $[N(V),N(V')]$ decays as $|\boldsymbol{x}-\boldsymbol{x}'|^{-4}$.

Proof The commutator $[N(V),N(V')]$ can be expanded as

$$\begin{aligned}
&[N(V),N(V')]\\
&\sim\sum_{ij=1}^{3}\int_V\mathrm{d}^3x\int_{V'}\mathrm{d}^3x'\,[(-\nabla^2)^{1/2}\delta_{ij}^{\perp}(\boldsymbol{x}-\boldsymbol{x}')]\\
&=\frac{1}{4\pi}\sum_{ij=1}^{3}\int_V\mathrm{d}^3x\int_{V'}\mathrm{d}^3x'\left[(-\nabla^2)^{1/2}\nabla_i\nabla_j\frac{1}{|\boldsymbol{x}-\boldsymbol{x}'|}\right] \qquad (16)
\end{aligned}$$

Here, we have employed (A-11) and subsequently applied the outcome derived in (15). In the latter, we determined that the initial term on the right-hand side of (A-11) holds no impact on the commutator, particularly when V and V' remain separate entities.

We now explicitly evaluate the integrand of (16) as follows:

$$\begin{aligned}
(-\nabla^2)^{1/2}\nabla_i\nabla_j\frac{1}{|\boldsymbol{x}-\boldsymbol{x}'|}&=\int\frac{\mathrm{d}^3k}{(2\pi)^3}\,k\,\mathcal{F}_{\boldsymbol{x}}\left\{\nabla_i\nabla_j\frac{1}{|\boldsymbol{x}-\boldsymbol{x}'|}\right\}\mathrm{e}^{\mathrm{i}\boldsymbol{k}\cdot\boldsymbol{x}}\\
&=\int\frac{\mathrm{d}^3k}{(2\pi)^3}\,k\,k_ik_j\mathcal{F}_{\boldsymbol{x}}\left\{\frac{1}{|\boldsymbol{x}-\boldsymbol{x}'|}\right\}\mathrm{e}^{\mathrm{i}\boldsymbol{k}\cdot\boldsymbol{x}}\\
&=\int\frac{\mathrm{d}^3k}{(2\pi)^3}\,k\,k_ik_j\mathcal{F}_{\boldsymbol{x}}\left\{\frac{1}{|\boldsymbol{x}|}\right\}\mathrm{e}^{\mathrm{i}\boldsymbol{k}\cdot\boldsymbol{x}}\mathrm{e}^{-\mathrm{i}\boldsymbol{k}\cdot\boldsymbol{x}'}\\
&=-4\pi\int\frac{\mathrm{d}^3k}{(2\pi)^3}\,\frac{k_ik_j}{k}\mathrm{e}^{\mathrm{i}\boldsymbol{k}\cdot\boldsymbol{x}}\mathrm{e}^{-\mathrm{i}\boldsymbol{k}\cdot\boldsymbol{x}'}\\
&=4\pi\nabla_i\nabla_j\int\frac{\mathrm{d}^3k}{(2\pi)^3}\,\frac{1}{k}\mathrm{e}^{\mathrm{i}\boldsymbol{k}\cdot(\boldsymbol{x}-\boldsymbol{x}')}\\
&=\frac{2}{\pi}\nabla_i\nabla_j\frac{1}{|\boldsymbol{x}-\boldsymbol{x}'|^2} \qquad (17)
\end{aligned}$$

For deriving the first equality, we utilized (A-12) and (A-13) after expanding them in the Fourier domain. For the second equality of (17) we used $\mathcal{F}\{\nabla_j f(\boldsymbol{x})\}=\mathrm{i}k_j\mathcal{F}\{f(\boldsymbol{x})\}$.[*7] For the third equality we applied the shift property of the Fourier transform. For the fourth equality, the Fourier transform pair $\mathcal{F}_{\boldsymbol{x}}\{|\boldsymbol{x}-\boldsymbol{x}'|^{-1}\}=4\pi/k^2$ was used. In the fifth equality we again applied $\mathcal{F}_{\boldsymbol{x}}\{\nabla_j f(\boldsymbol{k})\}=\mathrm{i}k_j f(\boldsymbol{k})$. Finally, to obtain the last equality we employed the Fourier transform pair $\mathcal{F}^{-1}\{k^{-1}\}=2\pi^2/|\boldsymbol{x}|^2$.[*8] Based on (16) and (17), we can infer that for $\boldsymbol{x}\neq\boldsymbol{x}'$, the commutator $[N(V),N(V')]$ asymptotically decays following a $|\boldsymbol{x}-\boldsymbol{x}'|^{-4}$ trend. □

The nonlocalizability of operator (4) was conjectured in [86], [100]. To the best of our knowledge the proof of Theorem 2 appears here for the first time. Theorem 3 is a new estimate of the size of the operator nonlocalizability.

The physical significance of Theorem 3 is that it provides an estimate of the size of nonlocalizability measured in terms of the separation $|\boldsymbol{x}-\boldsymbol{x}'|$. As the separation increases, the commutator, which measures the correlation of the local number density operator, decays slowly (i.e., not exponentially), suggesting a persistent, albeit small, non-negligible correlation. In the context of quantum beam optics, such persistent correlations have been discussed and found to be small for separations much larger than the wavelength. This is why photon emission can be considered approximately local for many applications [100], [105]. However, the viewpoint taken in this work is that the deviation from locality, while decaying with the separation $|\boldsymbol{x}-\boldsymbol{x}'|$, remains significant, especially for quantum information processing applications. Some of these applications may involve simultaneous measurements of two or more radiation field operators for optimal quantum state estimation or prediction, where the separation distance between two detec-

[*7] Recall that in this paper $\mathcal{F}\{f(\boldsymbol{x})\} := \int \mathrm{d}^3x\, f(\boldsymbol{x})\exp(-\mathrm{i}\boldsymbol{k}\cdot\boldsymbol{x})$ and $f(x)=\mathcal{F}^{-1}\{f(\boldsymbol{k})\} := \int\frac{\mathrm{d}^3k}{(2\pi)^3}\,f(\boldsymbol{k})\exp(\mathrm{i}\boldsymbol{k}\cdot\boldsymbol{x})$.
[*8] For derivation of all of these Fourier transforms relations used here, see [88], [104].

tors could be comparable to the wavelength, as in quantum microwave MIMO systems. In such scenarios, the commutators of the measurements, here directivity, which are not exactly zero, may contribute to the quality of the decision made at the receiver sites. For further related discussion, see the conclusion in Section V.

IV. Discussion and Examples

In this section, we provide a series of basic examples illustrating the computation and significance of the proposed formula for the directivity of a generic QSS. Note that here, as well as elsewhere in this paper, the density operator ρ appearing in (1) and other expressions is assumed to be known. In other words, the primary focus of this paper is on how a QSS with a known steady-state density operator can be characterized in terms of its directive properties in position space. Thus, the density operator ρ is the sole input data for the problem. The density operator ρ can be computed using various methods, including the quantum Langevin equations [86], [106], the Gorini-Kossakowski-Sudarshan-Lindblad (GKSL) master equation [64], [107], numerical solutions of the Schrödinger equation [7], numerical solutions of the Liouville-von Neumann equation [108], and others.[*9]

1. Single-mode QSS

Let's initially consider the highly specialized case where only one mode is emitted by the QSS.[*10] Its steady state density operator just prior to interaction with the detector is denoted as ρ. From (B-3), the single-mode positive-frequency component is given by

$$\boldsymbol{E}^{(+)}(\boldsymbol{x},t) = \hat{e}\,\mathrm{i}\sqrt{\hbar\omega_k/2\varepsilon_0 V}a\exp(\mathrm{i}\boldsymbol{k}\cdot\boldsymbol{x}-\mathrm{i}\omega t) \tag{18}$$

where $\hat{e}$ is the unit polarization vector of the single mode radiation field whose annihilation operator is a. A straightforward calculation of the directivity based on (1) yields

$$\mathcal{D}_q(|\boldsymbol{x}|,\Omega) = \mathrm{Tr}\{\rho\, a^\dagger a\}\left[\frac{1}{4\pi}\int_{4\pi}\mathrm{d}\Omega\,\mathrm{Tr}\{\rho\, a^\dagger a\}\right]^{-1} = 1 \tag{19}$$

which is independent of position $\boldsymbol{x}$ and time t. In simpler terms, irrespective of the specific values of $\boldsymbol{k}$ and the mode's polarization s, as prescribed in Definition 1, the single-mode QSS always demonstrates perfect isotropy, with the same value of directivity not only along all directions, but also at various radial positions.[*11] This outcome is indeed expected, as depicted in Figure 1(b), where the spacetime directivity holds a complementary relationship with the momentum space directivity depicted in Figure 1(a). In the context of the latter scenario, the directivity of a single mode naturally peaks in the directions aligned with the mode's wavevector $\boldsymbol{k}$. This contrast accentuates the inverse nature of spacetime and momentum space directivities. For a single-mode photon, the momentum is sharply defined, leading to completely indeterminate photon position. Consequently, the radiator's directivity in space becomes perfectly isotropic. Therefore, from the viewpoint of arriving at distinctive radiation properties, single-mode QSSs are trivial and not interesting. The minimum complexity necessary to achieve directive behavior is that of a two-mode system, which we will explore further next.

Let us note further that when considering a polarized atom, the directivity is typically higher due to the anisotropic nature of the radiation pattern. In such cases, a directivity value of 1.5 is often cited [110], [111]. This is because the radiation pattern of a polarized atom is not uniform in all directions, leading to higher directivity compared to an isotropic radiator. For an ensemble of atoms or emitters, the directivity tends to be lower due to the averaging effect, which smooths out the anisotropies present in single emitters. As a result, the directivity in such cases is closer to 1, reflecting a more isotropic radiation pattern. However, it must be emphasized that for dipole radiation, one is often dealing with a continuum of modes, not a single mode, such as in the phenomenon of resonance fluorescence radiation [79], [86], [112]. Therefore, quantum dipole radiation pertains to the topic in Section IV.3, which deals with scenarios involving a very large number of modes.

2. Two-mode QSS

Let us consider now the next level of complexity when two modes are radiated instead of one. First, we note that two-mode systems can be realized in cavity QED settings, where few modes can be excited and allowed to interact with a few localized objects such as atoms or quantum dots [81]. Consequently, one may consider the directivity results in this section as directly relevant to an experimentally realizable situation. In this setup, photons and atoms interact in a large box, and there is an interest in how a two-mode system of photons, properly excited, may become directed toward certain directions in space within this box.

Let the polarization and wavenumbers degrees of freedom associated with the two modes considered here be $\hat{e}_i$ and $\boldsymbol{k}_i$, where $i = 1,2$. The field is given by the linear sum

$$\begin{aligned}\boldsymbol{E}^{(+)}(\boldsymbol{x},t) = {}& \hat{e}_1\,\mathrm{i}\sqrt{\hbar\omega_{k_1}/2\varepsilon_0 V}a_1\mathrm{e}^{\mathrm{i}\boldsymbol{k}_1\cdot\boldsymbol{x}-\mathrm{i}\omega_{k_1}t} \\ & + \hat{e}_2\,\mathrm{i}\sqrt{\hbar\omega_{k_2}/2\varepsilon_0 V}a_2\mathrm{e}^{\mathrm{i}\boldsymbol{k}_2\cdot\boldsymbol{x}-\mathrm{i}\omega_{k_2}t}\end{aligned} \tag{20}$$

where $\hat{e}_i$ and a_i, $i = 1,2$, are the complex normalized polarization vectors and annihilation operators of the first and second modes, respectively, and we used the dispersion re-

[*9] For an example of using the GKSL master equation to numerically solve for ρ in momentum space, see [50], [55].
[*10] In this paper, the concept of mode refers to Fourier modes as defined in quantum electrodynamics and quantum optics, particularly illustrated in the expansions (A-3) and (A-4). Here, $\boldsymbol{k}$ and s are treated as a combined index $\kappa := (\boldsymbol{k}, s)$, see Appendix A. Therefore, when we mention one-mode or two-mode systems, we refer to $\kappa = 1$ or $\kappa = 2$, respectively. This indicates that achieving two modes (or more) can involve variations in either $\boldsymbol{k}$, s, or both.
[*11] The latter characteristics of the quantum case is in direct contrast to classical antennas where the directivity decays with position as $|\boldsymbol{x}|^{-2}$ [14], [71], [109].

lation $\omega = ck$, $k := |\boldsymbol{k}|$.[*12] To evaluate the quantum directivity of this two-mode system, we first compute the numerator of (1) as follows:

$$\begin{aligned}
&\mathrm{Tr}\left\{\rho \boldsymbol{E}^{(-)}(\boldsymbol{x},t)\cdot\boldsymbol{E}^{(+)}(\boldsymbol{x},t)\right\}\\
&\quad=\frac{\hbar c k_1}{2\varepsilon_0 V}\,\mathrm{Tr}\{\rho a_1^\dagger a_1\}+\frac{\hbar c k_2}{2\varepsilon_0 V}\,\mathrm{Tr}\{\rho a_2^\dagger a_2\}\\
&\qquad+\hat{e}_1^*\cdot\hat{e}_2\frac{\hbar c\sqrt{k_1k_2}}{2\varepsilon_0 V}\mathrm{Tr}\{\rho a_1^\dagger a_2\}\mathrm{e}^{\mathrm{i}(\boldsymbol{k}_2-\boldsymbol{k}_1)\cdot\boldsymbol{x}-\mathrm{i}c(k_2-k_1)t}\\
&\qquad+\hat{e}_2^*\cdot\hat{e}_1\frac{\hbar c\sqrt{k_1k_2}}{2\varepsilon_0 V}\mathrm{Tr}\{\rho a_2^\dagger a_1\}\mathrm{e}^{-\mathrm{i}(\boldsymbol{k}_2-\boldsymbol{k}_1)\cdot\boldsymbol{x}+\mathrm{i}c(k_2-k_1)t}
\end{aligned}\tag{21}$$

Next, the position vector is expanded in spherical coordinates as

$$\boldsymbol{x}=|\boldsymbol{x}|\hat{x}(\Omega),\quad \hat{x}(\Omega)=\hat{x}_1\cos\varphi\sin\theta+\hat{x}_2\sin\varphi\sin\theta+\hat{x}_3\cos\theta \tag{22}$$

Substituting (22) into (21) and integrating over all solid angles Ω, the ideal isotropic radiator reference, the denominator of (1), becomes $\frac{\hbar c}{2\varepsilon_0 V}\Gamma(|\boldsymbol{x}|)$ where

$$\begin{aligned}
\Gamma(|\boldsymbol{x}|)&:=k_1\mathrm{Tr}\{\rho a_1^\dagger a_1\}+k_2\mathrm{Tr}\{\rho a_2^\dagger a_2\}\\
&\quad+\frac{1}{4\pi}\sqrt{k_1k_2}\alpha_{12}\mathrm{e}^{-\mathrm{i}c(k_2-k_1)t}\int_{4\pi}\mathrm{d}\Omega\mathrm{e}^{\mathrm{i}(\boldsymbol{k}_2-\boldsymbol{k}_1)|\boldsymbol{x}|\cdot\hat{x}(\Omega)}\\
&\quad+\frac{1}{4\pi}\sqrt{k_1k_2}\alpha_{21}\mathrm{e}^{\mathrm{i}c(k_2-k_1)t}\int_{4\pi}\mathrm{d}\Omega\mathrm{e}^{-\mathrm{i}(\boldsymbol{k}_2-\boldsymbol{k}_1)|\boldsymbol{x}|\cdot\hat{x}(\Omega)}\\
&=k_1\alpha_{11}+k_2\alpha_{22}\\
&\quad+2\sqrt{k_1k_2}\mathrm{Re}\{\alpha_{12}\mathrm{e}^{-\mathrm{i}c(k_2-k_1)t}\}\frac{\sin(|\boldsymbol{x}||\boldsymbol{k}_1-\boldsymbol{k}_2|)}{|\boldsymbol{x}||\boldsymbol{k}_1-\boldsymbol{k}_2|}
\end{aligned}\tag{23}$$

In this context, the c-numbers α_{ij} are defined by

$$\alpha_{ij}:=\hat{e}_i^*\cdot\hat{e}_j\mathrm{Tr}\{\rho a_i^\dagger a_j\} \tag{24}$$

and are real for $i=j$, where in the latter case they indicate the number of photons in the ith mode within the radiation state ρ. For obtaining the last equality in (23) we used the identity [113]

$$\int_{4\pi}\mathrm{d}\Omega_k\,\mathrm{e}^{\mathrm{i}\boldsymbol{k}\cdot\boldsymbol{x}}=\int_{4\pi}\mathrm{d}\Omega_x\,\mathrm{e}^{\mathrm{i}\boldsymbol{k}\cdot\boldsymbol{x}}=4\pi\frac{\sin(|\boldsymbol{x}||\boldsymbol{k}|)}{|\boldsymbol{x}||\boldsymbol{k}|} \tag{25}$$

Finally, putting formulas (21) and (23) into (1) yields the following formula for the radiating two-mode quantum system:

$$\begin{aligned}
&\mathcal{D}_q(|\boldsymbol{x}|,\Omega,t)\\
&=\frac{\sum_{i=1}^2 k_i\alpha_{ii}+2(k_1k_2)^{\frac{1}{2}}\mathrm{Re}\{\alpha_{12}\mathrm{e}^{\mathrm{i}(\boldsymbol{k}_2-\boldsymbol{k}_1)|\boldsymbol{x}|\cdot\hat{x}(\Omega)-\mathrm{i}c(k_2-k_1)t}\}}{\sum_{i=1}^2 k_i\alpha_{ii}+2(k_1k_2)^{\frac{1}{2}}\mathrm{Re}\{\alpha_{12}\mathrm{e}^{-\mathrm{i}c(k_2-k_1)t}\}\frac{\sin(|\boldsymbol{x}||\boldsymbol{k}_1-\boldsymbol{k}_2|)}{|\boldsymbol{x}||\boldsymbol{k}_1-\boldsymbol{k}_2|}}
\end{aligned}\tag{26}$$

In writing the numerator of (26), we have made use of the symmetry relation $\alpha_{12}=\alpha_{21}^*$, which follows from the fact that ρ is a hermitian operator.

A couple of observations on the two-mode QSS's directivity formula (26) are in order. First, we note that for $\boldsymbol{k}_1=\boldsymbol{k}_2$, $\mathcal{D}_q(|\boldsymbol{x}|,\Omega,t)$ becomes independent of space and time, i.e., perfectly isotropic with directivity equal to 1, which is self consistent with what we have already established in Section IV.1 on single-mode QSSs.

Second, for $\boldsymbol{k}_1\neq\boldsymbol{k}_2$ but $k_1=k_2$, the directivity is a function of $\boldsymbol{x}$ but is independent of time. Third, from the limit $\lim_{|\boldsymbol{x}|\to\infty}\sin(|\boldsymbol{x}||\boldsymbol{k}_1-\boldsymbol{k}_2|)/|\boldsymbol{x}||\boldsymbol{k}_1-\boldsymbol{k}_2|=0$, we can deduce the maximum attainable directivity in the far-field zone as follows:

$$\max_{\Omega\in4\pi,t\in\mathbb{R}}\lim_{|\boldsymbol{x}|\to\infty}\mathcal{D}_q(|\boldsymbol{x}|,\Omega,t)=1+\frac{2\sqrt{k_1k_2}|\alpha_{12}|}{\sum_{i=1}^2 k_i\alpha_{ii}} \tag{27}$$

which is valid when $|\boldsymbol{x}|\gg\lambda_{\mathrm{eff}}$. Note that the matrix elements α_{ij} are not completely independent. For example, they must satisfy the inequality $\alpha_{11}^2+\alpha_{22}^2-2\Re\{\alpha_{12}\}>0$.[*13] In the special case when $\alpha_{11}=\alpha_{22}$, the maximal directivity becomes $1+(|\alpha_{12}|/\alpha_{11})\sqrt{k_1k_2}/[(k_1+k_2)/2]$. In other words, the two-mode directivity is maximized by those modes chosen such that the ratio between the geometric means of the wavenumbers, $\sqrt{k_1k_2}$, to the arithmetic mean, $(k_1+k_2)/2$, is maximized. Usually, this optimization problem must be solved under some constraints on the allowable values of k_1 and k_2.

Third, we note the appearance of the sinc function in (26). The sinc function, defined as $\mathrm{sinc}(x)=\sin(\pi x)/\pi x$ for $x\neq0$ and $\mathrm{sinc}(0)=1$, plays a crucial role in communications and information theory due to its intrinsic connection with several fundamental concepts such as correlation, filtering, and the Fourier transform. This relationship means that the sinc function describes an ideal low-pass filter, which perfectly passes all frequency components up to a certain cutoff frequency without distortion. In practical terms, this defines the theoretical limit of signal bandwidth and the ideal response of filters used in communication systems to eliminate unwanted frequencies. In the context in which it appears here, however, the sinc function plays the role of a spatial frequency-selective window, where the wavevector $\boldsymbol{k}$ represents spatial frequency. Thus, the sinc function acts as a spatial filter, limiting the wavelength components that may pass into the near- and far-field zones of the QSS by acting like a window in the $\boldsymbol{k}$-space filtering out very high $\boldsymbol{k}$ components (or very short wavelength components.)

An illustrative instance of a two-mode QSS is provided, where the wavevector of mode 2, denoted as $\boldsymbol{k}_2$, possesses a magnitude of k_0 and aligns along the x^3-direction. For mode 1, the wavevector $\boldsymbol{k}_1$, whose magnitude is also k_0,

[*12] The two modes may belong to the same $\boldsymbol{k}$, constituting then two orthonormal unit polarization vectors; or they may represent two total polarizations belonging to distinct modes in the $\boldsymbol{k}$-space. In the former case $\hat{e}_{1/2}$ are orthonormal, but in the latter case they need not be so.

[*13] For a proof, note that the operator $\boldsymbol{E}^{(-)}(\boldsymbol{x},t)\cdot\boldsymbol{E}^{(+)}(\boldsymbol{x},t)$ is positive semi-definite.

lies within the x^2x^3-plane and is oriented at an angle ϕ_0 with respect to the $\hat{x}_3$-axis. Figure 3 illustrates this radiating configuration with both momentum $\boldsymbol{k}$-space and position $\boldsymbol{x}$-space shown in the same figure. In general, the ratio $|\boldsymbol{k}_2|/|\boldsymbol{k}_1|$ and angle ϕ_0 are generic parameters that strongly influence the radiation pattern of the two-mode QSS.

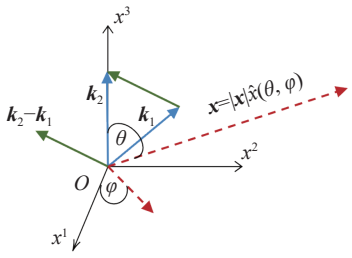


Figure 3 Abstract representation of a two-mode quantum source system. The two modes have wave vectors $\boldsymbol{k}_1$ and $\boldsymbol{k}_2$ confined to the x^2x^3 plane. The angle between $\boldsymbol{k}_1$ and $\boldsymbol{k}_2$ is ϕ_0 (not shown). The polarization vectors $\hat{e}_i$ are orthogonal to $\boldsymbol{k}_i$ for $i = 1,2$, respectively (not shown).

Motivated by the presence of the factor $\exp\{\mathrm{i}(\boldsymbol{k}_2 - \boldsymbol{k}_1)\cdot \boldsymbol{x}\}$, we define the effective wavelength of the two-mode system using

$$\lambda_{\text{eff}} := \frac{2\pi}{|\boldsymbol{k}_2 - \boldsymbol{k}_1|} \tag{28}$$

where the modes are characterized by wavevectors $\boldsymbol{k}_1$ and $\boldsymbol{k}_2$ as in (26). For instance, at a wavelength of $\lambda = 0.3$ μm with $|\boldsymbol{k}_1| = |\boldsymbol{k}_2|$ and an angle $\phi_0 = 30°$, we determine $\lambda_{\text{eff}}/\lambda = 1.93$. In general, the ratio $\lambda_{\text{eff}}/\lambda$ exhibits a significant dependency on the relative lengths of vectors $\boldsymbol{k}_1$ and $\boldsymbol{k}_2$, as well as the angle between them. The classification of the quantum radiation field as near or far field should be based on λ_{eff}. This example illustrates that the ratio $\lambda_{\text{eff}}/\lambda$ can be significant. Particularly, when vectors $\boldsymbol{k}_1$ and $\boldsymbol{k}_2$ are in close proximity, it is possible to observe $\lambda_{\text{eff}}/\lambda \gg 1$.

As a first example, we consider a pure coherent radiation state indexed by κ. The general form of this state is given by [80], [114]

$$|\alpha_\kappa\rangle = \mathrm{e}^{-\frac{1}{2}|\alpha_\kappa|^2} \sum_{n_\kappa=0}^{\infty} \frac{[\alpha_\kappa]^{n_\kappa}}{\sqrt{n_\kappa!}} |n_\kappa\rangle \tag{29}$$

This expansion is truncated to a finite dimension d. Let $|\alpha_1\rangle$ and $|\alpha_2\rangle$ be the two modes' states truncated to d each. We choose d for each mode depending on the values of $|\alpha_i|$, $i = 1,2$.[*14] The two-mode state is then given by $|\alpha\rangle = |\alpha_1\rangle|\alpha_2\rangle$ whose dimension is d^2. The density matrix for the pure two-mode coherent state system is then $\rho = |\alpha\rangle\langle\alpha|$. Similarly, for operators, if the annihilation operator in the mode space with dimension d (i.e., the Hilbert space $\mathbb{C}^d$) is denoted by a_m, then the annihilation operators of the two-mode system becomes $a_1 = a_m \otimes I_d$ and $a_1 = I_d \otimes a_m$, for modes 1 and 2, respectively, where I_d is the identity operator in $\mathbb{C}^d$. The dimensions of these operators are $d^2 \times d^2$.

For $\alpha_1 = 0.25$ and $\alpha_2 = 0.9$, it is found that $d = 10$ is enough to approximate the respective coherent states $|\alpha_1\rangle$ and $|\alpha_2\rangle$ in $\mathbb{C}^d$. The matrix elements in this case are $\alpha_{11} = 0.0625$, $\alpha_{22} = 0.8100$, and $\alpha_{12} = \alpha_{21} = 0.2250$, where we have chosen the polarization of the modes such that $\hat{e}_1^* \cdot \hat{e}_2 = 1$ (parallel polarization). We apply (26) to compute two angular directivity function plane sections at a distance of $5.43\lambda_{\text{eff}}$ from the origin. In Figure 4, the azimuthal directivity pattern for the $\theta = 0$ plane, $|\mathcal{D}_q(|\boldsymbol{x}|,\varphi,\theta = 0,t)|$, is depicted, which emerges as perfectly isotropic. This behavior is attributed to the fact that the $\theta = 0$ plane represents the $\hat{x}_1\hat{x}_3$-plane in this context, which encompasses one of the two modes' wavevectors, specifically $\boldsymbol{k}_2$. Consequently, the system effectively assumes a single-mode configuration, aligning with the previously established isotropy (cf. Section IV.1). We also present the $\theta = \pi/2$ plane of the directivity, denoted as $|\mathcal{D}_q(|\boldsymbol{x}|,\varphi,\theta = \pi/2,t)|$. This plane showcases a directive, nonisotropic pattern characterized by two primary lobes at angles $\varphi = 72°$ and $\varphi = 108°$, $\varphi = 252°$, and $\varphi = 290°$ along with multiple sidelobes and nulls evenly distributed across intermediate directions.

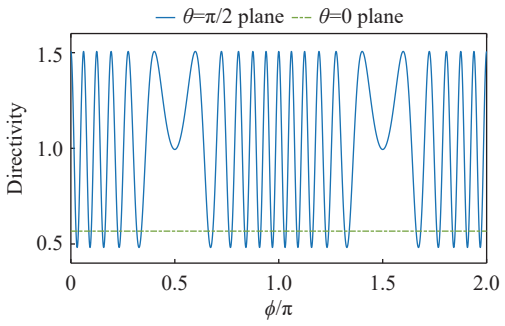


Figure 4 Azimuthal quantum directivity $|\mathcal{D}_q(|\boldsymbol{x}|,\Omega,t)|$ of a two-mode pure coherent state QSS with $\boldsymbol{k}_2 = k_0\hat{x}_3$ and $\boldsymbol{k}_1 = 4k_0[\sin(\phi_0)\hat{x}_2 + \cos(\phi_0)\hat{x}_3]$ and $\phi_0 = 30°$. The $\theta = 0$-plane is the $\hat{x}_1\hat{x}_3$-plane. Here, the two-mode quantum antenna coherent state $|\alpha\rangle = |0.25\rangle|0.9\rangle$ is characterized by the matrix elements $\alpha_{11} = 0.0625$, $\alpha_{22} = 0.8100$, and $\alpha_{12} = \alpha_{21} = 0.2250$. The angular pattern is evaluated at position $|\boldsymbol{x}| = 5.43\lambda_{\text{eff}} = 10.5\lambda$, where λ_{eff} is defined by (28), while $\lambda = 2\pi/k_0$. Time is evaluated at $t = T$, where $T = 2\pi/\omega_0$, $\omega_0 = 2\pi/k_0$.

The radiation state and polarization structure of this system are characterized by the elements of the Hermitian matrix α_{ij}, where i and j take values of 1 or 2. These values, detailed in the caption of Figure 4, essentially define the specific configuration of the two-mode QSS under examination. To demonstrate the significant influence of the QSS being studied on the radiation pattern's behavior, Figure 5 shows the directive radiation pattern of an alternative two-mode QSS. While this second QSS maintains the same parameters as presented in Figure 4, it incorporates slightly adjusted matrix elements α_{ij}. As depicted in the figure, the radiation pattern undergoes substantial modification. The

[*14] In general, we check that the norm of $|\alpha_i\rangle$ is unity. For larger values of $|\alpha_i|$, a bigger dimension d is needed.

peaks are no located at the directions $\varphi = 66.5°$, $\varphi = 113.4°$, $\varphi = 260°$, and $\varphi = 280°$. We note the loss of symmetry around the $\hat{x}_1\hat{x}_3$-plane and also the absense of deep null between the last two peaks. We also note that the maximumal directivity in the latter example is 1.8876, which is higher than 1.5067 for the example in Figure 4. This alteration indicates an enhanced directive characteristic. In essence, we infer that QSS configurations can be finely tuned to produce optimized radiation quantum states ρ and polarizations, resulting in the desired directive patterns.

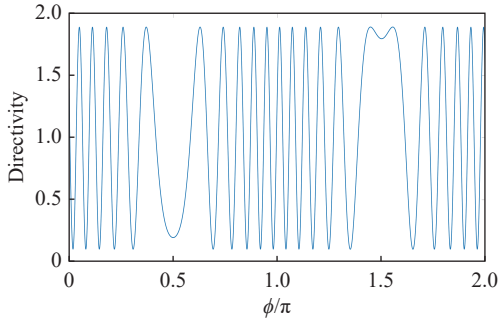


Figure 5 $\theta = \pi/2$ plane cut of the azimuthal quantum directivity $|\mathcal{D}_q(|\boldsymbol{x}|,\varphi,t)|$ of the two-mode QSS whose parameters are given in the caption of Figure 4. However, in this scenario, the two-mode coherent radiation state is $|\alpha\rangle = |0.25 + \mathrm{i}0.5\rangle|0.9\rangle$, with corresponding matrix elements $\alpha_{11} = 0.3125$, $\alpha_{22} = 0.8100$, and $\alpha_{12} = 0.2250 - \mathrm{i}0.4500$.

The impact of the observation distance from the origin is illustrated in Figure 6, where we depict the azimuthal quantum directivity in the $\theta = \pi/2$ plane at two distinct distances $|\boldsymbol{x}|$. At a distance of $|\boldsymbol{x}| = \lambda/2$, Figure 6 reveals a semblance reminiscent of an early embryonic stage of the pattern seen at larger distances. To validate this conceptual insight, we further focus on the angular directivity pattern at $|\boldsymbol{x}| = 2.5\lambda$ and $|\boldsymbol{x}| = 5\lambda$ observed around the angle $\varphi = 3\pi/2$, where we notice the gradual emergence of a peak. In general, on observation spheres characterized by larger radii, the radiation pattern tends to accumulate an increased count of alternating nulls and peaks, signifying concentrated sidelobes. This phenomenon can be comprehended by referencing (26). Upon close scrutiny of the numerator, it becomes

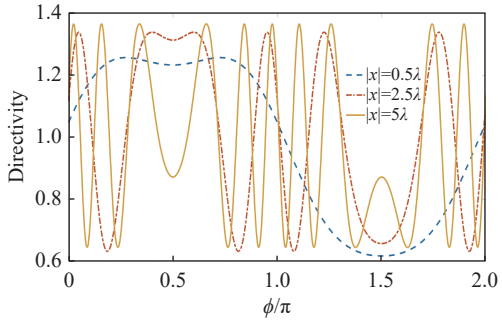


Figure 6 $\theta = \pi/2$ plane cut of the quantum directivity $|\mathcal{D}_q(|\boldsymbol{x}|,\varphi,t)|$ of the two-mode QSS whose parameters are given in Figure 4 evaluated at different distances from origin. Here, the two-mode coherent radiation state is $|\alpha\rangle = |1.25 + \mathrm{i}0.5\rangle|\mathrm{i}0.25\rangle$, with corresponding matrix elements $\alpha_{11} = 1.8123$, $\alpha_{22} = 0.0625$, and $\alpha_{12} = 0.1250 + \mathrm{i}0.3125$.

evident that amplified values of $|\boldsymbol{x}|$ correspond to heightened oscillatory behavior. As $|\boldsymbol{x}|$ attains significant magnitudes (relative to λ_{eff}), the intervals between successive maxima and minima, which are inversely proportional to $|\boldsymbol{x}|/\lambda_{\mathrm{eff}}$, diminish substantially, fostering a more complex oscillatory radiation pattern.

Finally, we now examine the maximal directivity of the QSS, a topic that is important for applications to quantum antennas and quantum sensors. In Figure 7, we numerically compute the maximum directivity for the system whose matrix α_{ij} is the same as in Figure 6. Note that the theoretical exact far-field upper bound (27) is 1.9484 in this case, which is in excellent agreement with the limit of the numerically computed directivity when $|\boldsymbol{x}| > \lambda$, i.e., in the far-field zone of the QSS. To reproduce the outcomes displayed in Figure 7, the quantum directivity formula (26) was executed a total of 129600 times. Despite the manageable duration for completing these calculations in the case of two-mode QSS, as the count of modes grows—reaching several hundreds and even beyond, for instance—determining the maximum directivity transforms into an exceedingly computationally intensive endeavor.

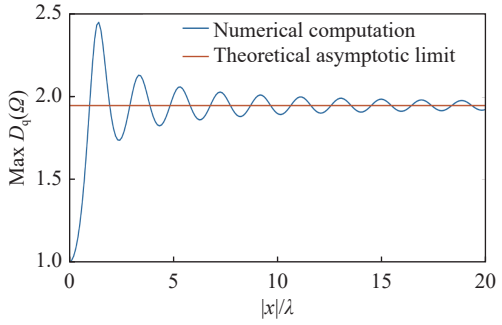


Figure 7 Maximal directivity $\max_{\Omega\in 4\pi}\mathcal{D}_q(|\boldsymbol{x}|,\Omega,t)$ numerically estimated for the QSS in Figure 6 but with variable $|\boldsymbol{x}|$. At each position $|\boldsymbol{x}|$, in order to numerically obtain maximization over all solid angles Ω, a total of 129600 angular points is generated in order to estimate the maximum directivity for 200 positions. The theoretical asymptotic limit is computed by means of (27).

To summarize, Figure 7 illustrates that a two-mode system possesses an inherent maximum directivity determined by the internal structure of the system, as described by (27). As the distance from the origin increases, the maximal directivity fluctuates around the theoretical asymptotic limit without stabilizing completely at the maximum (there are always small, gradually diminishing ripples around this limit). Note that in antenna theory, a common objective is to determine the maximal achievable directivity rather than analyzing directivity at every possible direction. This is precisely the focus of Figure 7.

3. Continuous-mode QSS

As seen above, the construction of a directive radiation pattern necessitates, at a minimum, a two-mode configuration. For higher-order mode systems, such as an N-mode system with $N > 2$, the methodology developed in Section IV.2 re-

mains applicable. Each *pair* of modes, denoted by indices ij with $i,j=1,2,\ldots,N$, functions akin to an "atom" contributing to the overall directivity. The comprehensive directive pattern results from the summation of these "atomic" pairwise contributions, with the QSS structure matrix given by (24). To ascend the complexity hierarchy, we now consider the arbitrary and general scenario where the number of modes is unconstrained and can be substantial or even infinite. In this context, pairs of modes are systematically incorporated, and their diverse contributions to the total directivity are orchestrated by the global quantum state ρ. This state assumes the role of a guiding coordinator for all contributing mode pairs.

To complete this presentation, we now give the general treatment for continuous-mode radiation. Using the complete general field operator expansion (B-3), the numerator of (1) can be put in the the following form:

$$\begin{aligned}&\mathrm{Tr}\{\rho \boldsymbol{E}^{(-)}(\boldsymbol{x},t)\cdot\boldsymbol{E}^{(+)}(\boldsymbol{x},t)\}\\&\quad=\frac{\hbar c}{2\varepsilon_0 V}\sum_{\boldsymbol{k}}\sum_{\boldsymbol{k}'}Q(\boldsymbol{k},\boldsymbol{k}')e^{\mathrm{i}(\boldsymbol{k}'-\boldsymbol{k})\cdot\boldsymbol{x}-\mathrm{i}c(k'-k)t}\end{aligned}\tag{30}$$

where

$$Q(\boldsymbol{k},\boldsymbol{k}'):=\sum_{ss'}(\hat{e}^{*}_{ks}\cdot\hat{\mathrm{e}}_{\mathrm{k}'s'})\sqrt{k_1k_2}\,\mathrm{Tr}\{\rho a^{\dagger}_{ks}a_{k's'}\}\tag{31}$$

Expression (30) can be reformulated by defining the $\boldsymbol{k}$-indexed array $\bar{y}(\boldsymbol{k};\boldsymbol{x},t):=[\exp(\mathrm{i}\boldsymbol{k}\cdot\boldsymbol{x}-\mathrm{i}ckt)]$, after which (30) can be rewritten as

$$\begin{aligned}&\mathrm{Tr}\left\{\rho \boldsymbol{E}^{(-)}(\boldsymbol{x},t)\cdot\boldsymbol{E}^{(+)}(\boldsymbol{x},t)\right\}\\&\quad=\frac{\hbar c}{2\varepsilon_0 V}\sum_{\boldsymbol{k}\boldsymbol{k}'}\bar{y}^{*}(\boldsymbol{k};\boldsymbol{x},t)Q(\boldsymbol{k},\boldsymbol{k}')\bar{y}(\boldsymbol{k}';\boldsymbol{x},t)\end{aligned}\tag{32}$$

It is straightforward to show that since ρ is a Hermitian operator then the matrix Q satisfies the symmetry condition $Q(\boldsymbol{k},\boldsymbol{k}')=Q^{*}(\boldsymbol{k}',\boldsymbol{k})$. Therefore, $Q(\boldsymbol{k},\boldsymbol{k}')$ is a Hermitian matrix and (32) is a Hermitian form.

Next, the denominator of (1) may be evaluated using the same method used in Section IV.2, yielding

$$\begin{aligned}&\frac{1}{4\pi}\int_{4\pi}\mathrm{d}\Omega\,\mathrm{Tr}\left\{\rho \boldsymbol{E}^{(-)}(\boldsymbol{x},t)\cdot\boldsymbol{E}^{(+)}(\boldsymbol{x},t)\right\}\\&\quad=\frac{\hbar c}{2\varepsilon_0 V}\sum_{\boldsymbol{k}}\sum_{\boldsymbol{k}'}Q(\boldsymbol{k},\boldsymbol{k}')\mathrm{e}^{-\mathrm{i}c(k'-k)t}\frac{\sin(|\boldsymbol{x}||\boldsymbol{k}-\boldsymbol{k}'|)}{|\boldsymbol{x}||\boldsymbol{k}-\boldsymbol{k}'|}\end{aligned}$$

where the identity (25) was utilized. Consequently inserting (30) and (33) into (1), the final quantum directivity expression becomes

$$\mathcal{D}_q(|\boldsymbol{x}|,\Omega,t)=\frac{\sum_{\boldsymbol{k}\boldsymbol{k}'}\bar{y}^{*}(\boldsymbol{k};\boldsymbol{x},t)Q(\boldsymbol{k},\boldsymbol{k}')\bar{y}(\boldsymbol{k}';\boldsymbol{x},t)}{\sum_{\boldsymbol{k}\boldsymbol{k}'}Q(\boldsymbol{k},\boldsymbol{k}')\dfrac{\sin(|\boldsymbol{x}||\boldsymbol{k}-\boldsymbol{k}'|)}{|\boldsymbol{x}||\boldsymbol{k}-\boldsymbol{k}'|}\mathrm{e}^{-\mathrm{i}c(k'-k)t}}\tag{33}$$

We can also take the limit of $V\to\infty$, transitioning to continuous-mode representation via the recipe $\int_{\mathbb{R}^3}\frac{\mathrm{d}^3k}{(2\pi)^3}\longleftrightarrow(1/V)\sum_{\boldsymbol{k}}$, leading to

$$\mathcal{D}_q(|\boldsymbol{x}|,\Omega,t)=\frac{\displaystyle\int\frac{\mathrm{d}^3k}{(2\pi)^3}\frac{\mathrm{d}^3k'}{(2\pi)^3}\bar{y}^{*}(\boldsymbol{k};\boldsymbol{x},t)Q(\boldsymbol{k},\boldsymbol{k}')\bar{y}(\boldsymbol{k}';\boldsymbol{x},t)}{\displaystyle\int\frac{\mathrm{d}^3k}{(2\pi)^3}\frac{\mathrm{d}^3k'}{(2\pi)^3}Q(\boldsymbol{k},\boldsymbol{k}')\frac{\sin(|\boldsymbol{x}||\boldsymbol{k}-\boldsymbol{k}'|)}{|\boldsymbol{x}||\boldsymbol{k}-\boldsymbol{k}'|}\mathrm{e}^{-\mathrm{i}c(k'-k)t}}\tag{34}$$

The discrete expression (33) has the advantage of being amenable to matrix analysis results pertinent to optimization [115], which is helpful for finding maximum (and minimum) directivity values [116]. On the other hand, the continuous form (34) can be useful for deriving closed form expressions since integrals are easier to evaluate than sums.

V. Concluding Remarks

An advantage of the directivity theory expounded within this paper is its capability to furnish a precise and rigorous characterization of a QSS. Indeed, a QSS finds its explicit definition as the minimal set of data required for the computation of the directivity (1). In this context, we delineate a QSS as a triad encompassing: 1) a collection of wave vectors $\boldsymbol{k}$, each associated with 2) a pair of polarization degrees, and 3) a Hermitian matrix $Q(\boldsymbol{k},\boldsymbol{k}')$ established by (31). Herein, the quantum state ρ becomes assimilated within the Hermitian matrix $Q(\boldsymbol{k},\boldsymbol{k}')$. Notably, ρ may exhibit time dependence akin to the interaction picture, but remains devoid of positional dependency. Hence, the quantum state of the QSS emerges as a global measure applicable across the entirety of the system. Conversely, when a localized insight into the system's behavior at specific positions is sought, the requisite information can be derived from Q through the utilization of (33) or (34).

Our investigation has revealed that the quantum directivity formula (1), rooted in photon detection theory, exhibits a nonlocal nature. To accommodate this characteristic, we have introduced a rigorous framework for characterizing nonlocalizable density operators, thereby enabling the exploration of how photons emitted by QSSs manifest localization in space. Our inquiry demonstrates that, akin to analogous constructs, the full localization of photons remains elusive. Nevertheless, explicit computations have demonstrated a noteworthy pattern: For two measurements conducted at spatial points $\boldsymbol{x}$ and $\boldsymbol{x}'$, the commutator of these measurements diminishes as $|\boldsymbol{x}-\boldsymbol{x}'|^{-4}$. Hence, in quantum information processing endeavors necessitating the simultaneous measurement of photonic fields at spatially disparate locales —examples being quantum multiple-input multiple-output (MIMO) communication systems and quantum multi-access links [31], [117]–[120]—it becomes imperative to account for the precise commutator value. In practical scenarios such as the design of optimal receivers for quantum MIMO channels, the commutator of photon counting rates emerges as an external constraint pivotal to the core of digital receiver design optimization [31]. Con-

versely, when the spatial separation between measurement sites expands considerably, one has the discretion to overlook the nonlocal attributes of the QSS. In such instances, our theory furnishes quantitative mechanisms to assess the error incurred by this decision.

Illustrative examples illustrating the proposed quantum directivity formula have unveiled a series of noteworthy structural features. It has been observed that single-mode QSSs inherently manifest perfect isotropy across space. Introducing a higher degree of complexity, the two-mode configuration surfaces as the minimal structure capable of rendering sophisticated directive characteristics. A multimode system with N modes produces a nonisotropic radiation pattern if and only if at least one of the diagonal matrix elements α_{ij}, $i \neq j$, $i,\ j = 1,2,\ldots,N$, is nonzero.

Several numerical examples were given to illustrate the case of two-mode systems. These examples were based on the use of pure coherent states within radiation fields. They demonstrated that, while all Fock states were excited, a distinctive angular directivity pattern emerged. This pattern was characterized by a zero photon counting rate in certain directions, contrasting with maximized rates in others. Moreover, the results emphasized the substantial impact of the wavevectors of the two modes on the radiation pattern, taking into account the angle between them and their amplitude ratio. Additionally, the observed radiation pattern underwent variations in shape with distance, eventually stabilizing at a steady-state asymptotic level of maximal directivity in the far zone. In sum, a pivotal observation was that the QSS directivity presented an intriguing and non-trivial optimization problem. Similar to classical antennas, it was illustrated that, for each observation sphere, both a maximum and minimum directivity existed for the system. Upon investigating these configurations, it was evident that despite their apparent simplicity, they can yield a diverse array of directive behaviors within space.

Subsequently, we progressed to treat the general scenario, accommodating an arbitrary number of modes. Detailed expressions were derived, spanning both discrete and continuous formulations. Evidently, the presented theory facilitates efficient computations of maximal directivity, particularly when the number of modes remains modest. However, in instances involving a substantial count of modes, we advocate recourse to the theorems governing the maximization of Hermitian forms within matrix analysis. This recommendation stems from the realization that our directivity formulation can be cast in such forms, offering a strategic approach for large-scale mode scenarios.

Appendix A. Free Field Quantization

The total electric vector potential and electric field operators, labeled by the position $\boldsymbol{x} \in \mathbb{R}^3$, are expanded as

$$\boldsymbol{A}(\boldsymbol{x}) = \boldsymbol{A}^{(+)}(\boldsymbol{x}) + \boldsymbol{A}^{(-)}(\boldsymbol{x}) \tag{A-1}$$

$$\boldsymbol{E}(\boldsymbol{x}) = \boldsymbol{E}^{(+)}(\boldsymbol{x}) + \boldsymbol{E}^{(-)}(\boldsymbol{x}) \tag{A-2}$$

respectively. The superscripts $(\pm)$ denotes the positive/negative frequency components, respectively, while $\boldsymbol{A}^{(-)}(\boldsymbol{x}) = \boldsymbol{A}^{(+)\dagger}(\boldsymbol{x})$, $\boldsymbol{E}^{(-)}(\boldsymbol{x}) = \boldsymbol{E}^{(+)\dagger}(\boldsymbol{x})$. In box mode quantization, the field operators expansions are

$$\boldsymbol{A}^{(+)}(\boldsymbol{x}) = \sum_{ks} \hat{e}_{ks} \sqrt{\frac{\hbar}{2\varepsilon_0 \omega_k V}} a_{ks} \mathrm{e}^{\mathrm{i}\boldsymbol{k}\cdot\boldsymbol{x}} \tag{A-3}$$

$$\boldsymbol{E}^{(+)}(\boldsymbol{x}) = \sum_{ks} \hat{e}_{ks} \mathrm{i} \sqrt{\frac{\hbar\omega_k}{2\varepsilon_0 V}} a_{ks} \mathrm{e}^{\mathrm{i}\boldsymbol{k}\cdot\boldsymbol{x}} \tag{A-4}$$

where $\boldsymbol{k}$ is the (periodic boundary conditioned) box quantization wavevector; V is the box volume; $\omega_k = ck$ is the k-th mode frequency with $k := |\boldsymbol{k}|$, while c is the vacuum speed of light; $s \in \{0,1\}$ labels the polarization (orthonormal) set $\hat{e}_{ks}$; and a_{ks} is the ks-th mode annihilation operator.

Here, the electromagnetic boundary condition we work with is the periodic boundary condition, leading to the discrete version known as the box quantization scheme where continuous integrals and mode indices are discretized and the fields are confined into within a box of volume V [63], [86], [106], [121]. This motivates our subsequent use of the shorthand expression $\kappa := (\boldsymbol{k}, s) := (n_1, n_2, n_3; s)$, where $n_1, n_2, n_3 \in \mathbb{Z}$ are integers describing the periodic boundary condition along three orthogonal Cartesian directions for the purpose of labeling bosonic modes. With a slight abuse of notation, we treat the two vectors $\boldsymbol{k}$ and (n_1, n_2, n_3) as more or less the same and freely write expressions such as $\boldsymbol{k} \in \mathbb{Z}^3$ or $\boldsymbol{k}s \in \mathbb{Z}^3 \times \{1,2\}$ in the box quantization case.

The relation between the positive frequency components of the electric field and the vector potential is given by

$$\boldsymbol{E}^{(+)}(\boldsymbol{x}) = \mathrm{i}c(-\nabla^2)^{1/2} \boldsymbol{A}^{(+)}(\boldsymbol{x}) \tag{A-5}$$

Note that we employ the operator $(-\nabla^2)^{1/2}$, rigorously defined by (A-12) and (A-13) provided below. The utilization of this operator is crucial for computing field/field commutators in quantum electrodynamics. Significantly, it substantially reduces the labor required for performing the inverse Fourier transformation operation in space [63], [110]. This operator enables effective work in space-time, eliminating the need to continually shift between position and momentum spaces. The following commutation relations are valid in vacuum [110]:

$$\left[A_i^{(+)}(\boldsymbol{x}), A_j^{(-)}(\boldsymbol{x}')\right] = \frac{\hbar}{2\epsilon_0 c}(-\nabla^2)^{-1/2} \delta_{ij}^{\perp}(\boldsymbol{x} - \boldsymbol{x}') \tag{A-6}$$

$$\left[E_i^{(+)}(\boldsymbol{x}), E_j^{(-)}(\boldsymbol{x}')\right] = \frac{\hbar c}{2\epsilon_0}(-\nabla^2)^{1/2} \delta_{ij}^{\perp}(\boldsymbol{x} - \boldsymbol{x}') \tag{A-7}$$

$$\left[A_i^{(+)}(\boldsymbol{x}), A_j^{(+)}(\boldsymbol{x}')\right] = \left[A_i^{(-)}(\boldsymbol{x}), A_j^{(-)}(\boldsymbol{x}')\right] = 0 \tag{A-8}$$

$$\left[E_i^{(+)}(\boldsymbol{x}), E_j^{(+)}(\boldsymbol{x}')\right] = \left[E_i^{(-)}(\boldsymbol{x}), E_j^{(-)}(\boldsymbol{x}')\right] = 0 \tag{A-9}$$

where we note that these relations hold for all $i, j = 1,2,3$. The transverse Dirac delta function used above is defined by

$$\delta_{ij}^{\perp}(\boldsymbol{x} - \boldsymbol{x}') := \int \frac{\mathrm{d}^3 k}{(2\pi)^3} \left[\delta_{ij} - \frac{k_i k_j}{k^2}\right] \mathrm{e}^{\mathrm{i}\boldsymbol{k}\cdot(\boldsymbol{x}-\boldsymbol{x}')} \tag{A-10}$$

Furthermore, it can be shown that [110]

$$\delta_{ij}^{\perp}(\boldsymbol{x} - \boldsymbol{x}') = \delta_{ij}\delta(x - x') + \frac{1}{4\pi}\nabla_i \nabla_j \frac{1}{|\boldsymbol{x} - \boldsymbol{x}'|} \tag{A-11}$$

Differential operators in the form $(-\nabla^2)^{\pm 1/2}$ can best be defined by

$$g(-\nabla^2)F(\boldsymbol{x}) := \int \mathrm{d}^3 x'\ G_g(\boldsymbol{x} - \boldsymbol{x}')F(\boldsymbol{x}') \tag{A-12}$$

where

$$G_g(\boldsymbol{x}-\boldsymbol{x}') := \int \frac{\mathrm{d}^3x}{(2\pi)^3} g\left(k^2\right) \mathrm{e}^{\mathrm{i}\boldsymbol{k}\cdot(\boldsymbol{x}-\boldsymbol{x}')} \tag{A-13}$$

This definition is valid for any measurable function $g(\cdot)$. For example, the special case $g(-\nabla^2)\exp(\mathrm{i}\boldsymbol{k}\cdot\boldsymbol{x}) = g(k^2)\exp(\mathrm{i}\boldsymbol{k}\cdot\boldsymbol{x})$ is important. Note that the operator $g(-\nabla^2)$ can be moved to the right through the following useful integration by parts identity:

$$\int \mathrm{d}^3x F_1^*(\boldsymbol{x}) g\left(-\nabla^2\right) F_2(\boldsymbol{x}) = \int \mathrm{d}^3x \left[g(-\nabla^2)F_1^*(\boldsymbol{x})\right] F_2(\boldsymbol{x}) \tag{A-14}$$

where $F_1(\boldsymbol{x})$ and $F_2(\boldsymbol{x})$ are two generic functions.

Appendix B. Photon Detection Theory

In quantum optics, photodiodes and other devices are systematically deployed in order to perform local measurements of the radiation fields [78], [122], [123]. If the detector can be assumed to be localized at a single point $\boldsymbol{x}$ in the QSS's exterior domain $\mathcal{D}_{\mathrm{ex}}$, then the signal outputed by the detector may be interpreted as a preliminary representation of the configuration of the quantum field at that spatial location [80]. For example, here we will focus on single counting statistics, which can be captured by the position-dependent signal [78]

$$w(\boldsymbol{x},t) := \mathrm{Tr}\{\rho \boldsymbol{E}^{(-)}(\boldsymbol{x},t)\cdot\boldsymbol{E}^{(+)}(\boldsymbol{x},t)\} \tag{B-1}$$

where the time-dependent operators (interaction picture) are given by [79]

$$\boldsymbol{A}^{(+)}(\boldsymbol{x},t) = \sum_{\boldsymbol{ks}} \hat{e}_{\boldsymbol{ks}} \sqrt{\frac{\hbar}{2\varepsilon_0\omega_k V}} a_{\boldsymbol{ks}} \mathrm{e}^{\mathrm{i}\boldsymbol{k}\cdot\boldsymbol{x}-\mathrm{i}\omega_k t} \tag{B-2}$$

$$\boldsymbol{E}^{(+)}(\boldsymbol{x},t) = \sum_{\boldsymbol{ks}} \hat{e}_{\boldsymbol{ks}} \mathrm{i} \sqrt{\frac{\hbar\omega_k}{2\varepsilon_0 V}} a_{\boldsymbol{ks}} \mathrm{e}^{\mathrm{i}\boldsymbol{k}\cdot\boldsymbol{x}-i\omega_k t} \tag{B-3}$$

The density operator of the system, ρ, is the reduced radiation density operator obtained in the steady state after tracing out all the matter degrees of freedom in the QSS operator $\boldsymbol{J}(\boldsymbol{x})$ (see Figure 1) [55]. It represents the statistical mixture of all initial radiation field states entering into interaction with the photon detector [63].

In order to understand the physical meaning of the signal (B-1), we quickly recap quantum detection theory in quantum optics [78], [80], [124]. Recall that using perturbation theory, one can compute the total probability of all atomic transitions from lower states to excited stated after interaction with the illumination (measured) electromagnetic field using the following formula [78]:

$$p(\boldsymbol{x},t) = \sum_{ij} \int_{t_0}^{t} \mathrm{d}t_1 \int_{t_0}^{t} \mathrm{d}t_2\, D_{ij}(t_1-t_2) G_{ij}^{(1)}(\boldsymbol{x},t_1;\boldsymbol{x},t_2) \tag{B-4}$$

where the spatiotemporal field-field correlation tensor $G_{ij}^{(1)}$ is defined by

$$G_{ij}^{(1)}(\boldsymbol{x},t_1;\boldsymbol{x},t_2) := \mathrm{Tr}\{\rho E_i^{(-)}(\boldsymbol{x},t_1) E_j^{(+)}(\boldsymbol{x},t_2)\} \tag{B-5}$$

The tensor $D_{ij}: \mathbb{R} \to \mathbb{C}^3 \times \mathbb{C}^3$ appearing in (B-4) represents the photodetector impulse response and is a unique characterization of each device, sometimes referred to as sensitivity function.[*B1] The single photon counting rate $w(\boldsymbol{x},t)$ is then defined as the counting rate $w^{(1)}(\boldsymbol{x},t) := \mathrm{d}p(\boldsymbol{x},t)/\mathrm{d}t$. Using (B-4), this becomes

$$w^{(1)}(\boldsymbol{x},t) = 2\mathrm{Re} \sum_{ij} \int_{t_0}^{t} \mathrm{d}t'\, D_{ij}(t'-t) G_{ij}^{(1)}(\boldsymbol{x},t';\boldsymbol{x},t) \tag{B-6}$$

Consider now the special Fourier transform defined by $X_{ij}(\omega,t) := \int_{t_0}^{t} \mathrm{d}t' G_{ij}^{(1)}(\boldsymbol{x},t';\boldsymbol{x},t)\exp[\mathrm{i}\omega(t-t')]$. Let its bandwidth be B_X. We may then rewrite (B-6) as

$$w^{(1)}(\boldsymbol{x},t) = 2\mathrm{Re} \sum_{ij} \int \frac{\mathrm{d}\omega}{2\pi} D_{ij}(\omega) X_{ij}(\omega,t) \tag{B-7}$$

where $D_{ij}(\omega) := \mathcal{F}_\tau\{D_{ij}(\tau)\}$ is the Fourier transform of the detector impulse response (spectral device sensitivity function). In general, if the coherence time of the field is T_c, then $B_X \sim 1/T_c$ since the observation time $\Delta t := t - t_0$ satisfies $\Delta t \gg T_c$. Now let the device sensitivity bandwidth be B_D, which is defined as the effective bandwidth of the function $\|D_{ij}(\omega)\|$, where $\|\cdot\|$ is a suitable matrix or tensor norm. Then we say our measurement of the radiation field is a broadband measurement if the condition $B_D \gg B_X$ holds. In that case, it can be shown that (B-7) may be reduced to the considerably simpler relation [80]

$$w^{(1)}(\boldsymbol{x},t) = \sum_{ij} D_{ij} G_{ij}^{(1)}(\boldsymbol{x},t;\boldsymbol{x},t) \tag{B-8}$$

where D_{ij} is now a constant device (sensitivity) tensor.[*B2] We may also expand the hermitian tensor D_{ij} as a Hermitian matrix in the form $\sum_{n=1}^{3} D_n u_{ni} u^*_{nj}$, where $\hat{u}_n, n = 1,2,3$, are orthonormal vectors. Using this form in (B-8), we obtain

$$w^{(1)}(\boldsymbol{x},t) = \sum_{n=1}^{3} D_n G_n^{(1)}(\boldsymbol{x},t;\boldsymbol{x},t) \tag{B-9}$$

where

$$G_n^{(1)}(\boldsymbol{x},t;\boldsymbol{x},t) := \mathrm{Tr}\left\{\rho\, \hat{u}_n \cdot \boldsymbol{E}^{(-)}(\boldsymbol{x},t)\, \boldsymbol{E}^{(+)}(\boldsymbol{x},t)\cdot\hat{u}_n^*\right\} \tag{B-10}$$

Expression (B-9) proves to be highly advantageous for practical applications due to its ability to break down the counting rate into three distinct preferred spatial directions. This becomes particularly useful when considering scenarios involving the incorporation of a polarizer within the photodetection process. Such a setup allows for the precise measurement of quantum observables along specified spatial directions. In the special case when $D_1 = D_2 = D_3 = D$, the expression (B-9) maybe reduced then to

$$w^{(1)}(\boldsymbol{x},t) = D\mathrm{Tr}\left\{\rho \boldsymbol{E}^{(-)}(\boldsymbol{x},t)\cdot\boldsymbol{E}^{(+)}(\boldsymbol{x},t)\right\} \tag{B-11}$$

If we define $w(\boldsymbol{x},t) := w^{(1)}(\boldsymbol{x},t)/D$, then the signal introduced in (B-1) is reproduced. In summary, $w(\boldsymbol{x},t)$ represents the rate of single-photon detection at time t when a localized point-like photodetector is positioned at $\boldsymbol{x}$. The photodetector's response exhibits isotropy in space, with sensitivity D along all directions. This rate is now normalized with respect to D.

Appendix C. Mandel's Detection Theory

Using the identity $(-\nabla^2)^{1/2} = (-\nabla^2)^{1/4}(-\nabla^2)^{1/4}$, the local number operator is defined by the expression as follows [102]:

$$N(V) = \int_{\boldsymbol{x}\in V} \mathrm{d}^3x\, \boldsymbol{M}^\dagger(\boldsymbol{x})\cdot\boldsymbol{M}(\boldsymbol{x}) \tag{C-1}$$

[*B1] This tenor enjoys the important Hermitian symmetry condition $D_{ij}(t) = D_{ji}^*(-t)$.

[*B2] Note that in deriving (B-8), the symmetry properties of D_{ij} and $G_{ij}^{(1)}$ were used in addition to the one-sided sifting property of the Dirac delta function.

where

$$\boldsymbol{M}(\boldsymbol{x}) := -\mathrm{i}\sqrt{\frac{2\varepsilon_0}{\hbar c}}\left(-\nabla^2\right)^{1/4}\boldsymbol{E}^{(+)}(\boldsymbol{x}) \tag{C-2}$$

is referred to as Mandel's detection operator. It is evident that the local operator in (C-1) is positive semidefinite. However, as can be demonstrated, it is nonlocalizable, consistent with other photon operators in electromagnetism. A definition of directivity based on Mandel's detection operator is the following:

$$\mathcal{D}_{\mathrm{M}} := \frac{\mathrm{Tr}\left\{\rho(-\nabla^2)^{1/4}\boldsymbol{E}^{(-)}\cdot(-\nabla^2)^{1/4}\boldsymbol{E}^{(+)}\right\}}{\frac{1}{4\pi}\int_{4\pi}\mathrm{d}\Omega\,\mathrm{Tr}\left\{\rho(-\nabla^2)^{1/4}\boldsymbol{E}^{(-)}\cdot(-\nabla^2)^{1/4}\boldsymbol{E}^{(+)}\right\}} \tag{C-3}$$

It should be noted that (C-3) was not derived by Mandel and, to the best of our knowledge, is presented here for the first time, much like Definition 1.

References

[1] W. E. I. Sha, A. Y. Liu, and W. C. Chew, "Dissipative quantum electromagnetics," *IEEE Journal on Multiscale and Multiphysics Computational Techniques*, vol. 3, pp. 198–213, 2018.

[2] W. C. Chew, W. E. I. Sha, and Q. I. Dai, "Green's dyadic, spectral function, local density of states, and fluctuation dissipation theorem," *Progress in Electromagnetics Research*, vol. 166, pp. 147–165, 2019.

[3] D. Y. Na and W. C. Chew, "Classical and quantum electromagnetic interferences: What is the difference?," *Progress in Electromagnetics Research*, vol. 168, pp. 1–13, 2020.

[4] W. C. Chew, A. Y. Liu, C. Salazar-Lazaro, *et al*., "Quantum electromagnetics: A new look—Part I," *IEEE Journal on Multiscale and Multiphysics Computational Techniques*, vol. 1, pp. 73–84, 2016.

[5] W. C. Chew, A. Y. Liu, C. Salazar-Lazaro, *et al*., "Quantum electromagnetics: A new look—Part II," *IEEE Journal on Multiscale and Multiphysics Computational Techniques*, vol. 1, pp. 85–97, 2016.

[6] T. E. Roth and W. C. Chew, "Role of classical time domain CEM methods for quantum electromagnetics," in *Proceedings of the 2019 IEEE International Symposium on Antennas and Propagation and USNC-URSI Radio Science Meeting*, Atlanta, GA, USA, pp. 1063–1064, 2019.

[7] D. Y. Na, J. Zhu, W. C. Chew, *et al*., "Quantum information preserving computational electromagnetics," *Physical Review A*, vol. 102, no. 1, article no. 013711, 2020.

[8] S. A. Schelkunoff, "A mathematical theory of linear arrays," *The Bell System Technical Journal*, vol. 22, no. 1, pp. 80–107, 1943.

[9] L. B. Felsen and N. Marcuvitz, *Radiation and Scattering of Waves*. IEEE Press, Piscataway, NJ, USA, 1994.

[10] D. Bohm, *Quantum Theory*. Dover Publications, New York, NY, USA, 1989.

[11] P. A. M. Dirac, *The Principles of Quantum Mechanics*, 4th ed., Oxford University Press, Oxford, UK, 1981.

[12] J. von Neumann, *Mathematical Foundations of Quantum Mechanics*. R. T. Beyer, trans. Princeton University Press, Princeton, NJ, USA, 2018.

[13] S. A. Schelkunoff and H. T. Friis, *Antennas: Theory and Practice*. Chapman & Hall, London, UK, 1952.

[14] C. A. Balanis, *Antenna Theory: Analysis and Design*, 4th ed., Wiley, Hoboken, NJ, USA, 2015.

[15] G. Y. Slepyan and A. Boag, "Quantum nonreciprocity of nanoscale antenna arrays in timed Dicke states," *Physical Review Letters*, vol. 111, no. 2, article no. 023602, 2013.

[16] G. Y. Slepyan, S. Vlasenko, and D. Mogilevtsev, "Quantum antennas," *Advanced Quantum Technologies*, vol. 3, no. 4, article no. 1900120, 2020.

[17] G. Slepyan and A. Boag, "Super-operator linear equations and their applications to quantum antennas and quantum light scattering," *Applied Sciences*, vol. 12, no. 17, article no. 8498, 2022.

[18] N. Aslam, H. Y. Zhou, E. K. Urbach, *et al*., "Quantum sensors for biomedical applications," *Nature Reviews Physics*, vol. 5, no. 3, pp. 157–169, 2023.

[19] L. J. Fiderer and D. Braun, "Quantum metrology with quantum-chaotic sensors," *Nature Communications*, vol. 9, no. 1, article no. 1351, 2018.

[20] Y. Xia, A. R. Agrawal, C. M. Pluchar, *et al*., "Entanglement-enhanced optomechanical sensing," *Nature Photonics*, vol. 17, no. 6, pp. 470–477, 2023.

[21] X. D. Chen, E. H. Wang, L. K. Shan, *et al*., "Quantum enhanced radio detection and ranging with solid spins," *Nature Communications*, vol. 14, no. 1, article no. 1288, 2023.

[22] G. Slepyan, S. Vlasenko, D. Mogilevtsev, *et al*., "Quantum radars and lidars: Concepts, realizations, and perspectives," *IEEE Antennas and Propagation Magazine*, vol. 64, no. 1, pp. 16–26, 2022.

[23] I. Liberal and R. W. Ziolkowski, "Quantum antenna arrays," in *Antenna and Array Technologies for Future Wireless Ecosystems*, Y. J. Guo and R. W. Ziolkowski, Eds. Wiley, New York, NY, USA, pp. 419–446, 2022.

[24] C. Schimpf, M. Reindl, F. Basso Basset, *et al*., "Quantum dots as potential sources of strongly entangled photons: Perspectives and challenges for applications in quantum networks," *Applied Physics Letters*, vol. 118, no. 10, article no. 100502, 2021.

[25] G. Slepyan, A. Boag, V. Mordachev, *et al*., "Anomalous electromagnetic coupling via entanglement at the nanoscale," *New Journal of Physics*, vol. 19, no. 2, article no. 023014, 2017.

[26] M. Hensen, T. Heilpern, S. K. Gray, *et al*., "Strong coupling and entanglement of quantum emitters embedded in a nanoantenna-enhanced plasmonic cavity," *ACS Photonics*, vol. 5, no. 1, pp. 240–248, 2018.

[27] M. Moreno-Cardoner, R. Holzinger, and H. Ritsch, "Efficient nano-photonic antennas based on dark states in quantum emitter rings," *Optics Express*, vol. 30, no. 7, pp. 10779–10791, 2022.

[28] S. Mokhlespour, J. E. M. Haverkort, G. Slepyan, *et al*., "Collective spontaneous emission in coupled quantum dots: Physical mechanism of quantum nanoantenna," *Physical Review B*, vol. 86, no. 24, article no. 245322, 2012.

[29] H. R. Haakh and D. Martín-Cano, "Squeezed light from entangled nonidentical emitters via nanophotonic environments," *ACS Photonics*, vol. 2, no. 12, pp. 1686–1691, 2015.

[30] V. Sandoghdar, M. Agio, X. W. Chen, *et al*., "7-antennas, quantum optics and near-field microscopy: From part I - FUNDAMENTALS," in *Optical Antennas*, M. Agio and A. Alù, Eds. Cambridge University Press, Cambridge, UK, 2013.

[31] S. Mikki, "A quantum MIMO architecture for antenna wireless digital communications," *Progress in Electromagnetics Research C*, vol. 93, pp. 143–156, 2019.

[32] S. Mikki and M. Herde, "Analysis and design of secure quantum communication systems utilizing electromagnetic Schrodinger coherent states," *Quantum Engineering*, vol. 3, no. 3, article no. e72, 2021.

[33] D. A. Broadway, N. Dontschuk, A. Tsai, *et al*., "Spatial mapping of band bending in semiconductor devices using in situ quantum sensors," *Nature Electronics*, vol. 1, no. 9, pp. 502–507, 2018.

[34] S. Mikki, "Quantum antenna theory for secure wireless communications," in *Proceedings of the 14th European Conference on Antennas and Propagation (EuCAP)*, Copenhagen, Denmark, pp. 1–4, 2020.

[35] L. Shi, Z. Li, M. Chen, *et al*., "Quantum effect-based flexible and transparent pressure sensors with ultrahigh sensitivity and sensing density," *Nature Communications*, vol. 11, no. 1, article no. 3529, 2020.

[36] S. Mikki, "Fundamental spacetime representations of quantum antenna systems," *Foundations*, vol. 2, no. 1, pp. 251–289, 2022.

[37] P. Georgi, M. Massaro, K. H. Luo, *et al*., "Metasurface interferometry toward quantum sensors," *Light: Science & Applications*, vol. 8, no. 1, article no. 70, 2019.

[38] A. Mikhalychev, D. Mogilevtsev, G. Y. Slepyan, *et al*., "Synthesis of quantum antennas for shaping field correlations," *Physical Review Applied*, vol. 9, no. 2, article no. 024021, 2018.

[39] R. Filter, S. Muhlig, T. Eichelkraut, *et al*., "Controlling the dynamics of quantum mechanical systems sustaining dipole-forbidden transitions via optical nanoantennas," *Physical Review B*, vol. 86, no. 3, article no. 035404, 2012.

[40] J. F. Liu, M. Zhou, L. Ying, *et al*., "Enhancing the optical cross section of quantum antenna," *Physical Review A*, vol. 95, no. 1, article no. 013814, 2017.

[41] R. Esteban, A. G. Borisov, P. Nordlander, *et al*., "Bridging quantum and classical plasmonics with a quantum-corrected model," *Nature Communications*, vol. 3, no. 1, article no. 825, 2012.

[42] P. E. Kremer, A. C. Dada, P. Kumar, *et al*., "Strain-tunable quantum dot embedded in a nanowire antenna," *Physical Review B*, vol. 90, no. 20, article no. 201408(R), 2014.

[43] I. Liberal, I. Ederra, and R. W. Ziolkowski, "Quantum antenna arrays: The role of quantum interference on direction-dependent photon statistics," *Physical Review A*, vol. 97, no. 5, article no. 053847, 2018.

[44] I. Liberal, I. Ederra, and R. W. Ziolkowski, "Control of a quantum emitter's bandwidth by managing its reactive power," *Physical Review A*, vol. 100, no. 2, article no. 023830, 2019.

[45] Z. A. Peng, G. Q. Yang, G. M. Huang, *et al*., "Directional nonclassicality of resonance fluorescence from a three-body quantum antenna via geometry-dependent frequency engineering," *Physical Review A*, vol. 102, no. 5, article no. 053715, 2020.

[46] H. Giessen and M. Lippitz, "Directing light emission from quantum dots," *Science*, vol. 329, no. 5994, pp. 910–911, 2010.

[47] T. Grosjean, M. Mivelle, G. W. Burr, *et al*., "Optical horn antennas for efficiently transferring photons from a quantum emitter to a single-mode optical fiber," *Optics Express*, vol. 21, no. 2, pp. 1762–1772, 2013.

[48] R. Hernandez, P. R. Wiecha, J. M. Poumirol, *et al*., "Directional silicon nano-antennas for quantum emitter control designed by evolutionary optimization," *Journal of the Optical Society of America B*, vol. 41, no. 2, pp. A108–A115, 2024.

[49] I. Liberal, I. Ederra, and R. W. Ziolkowski, "Grating lobes in higher-order correlation functions of arrays of quantum emitters: Directional photon bunching versus correlated directions," *Photonics*, vol. 6, no. 1, article no. 14, 2019.

[50] S. Mikki, "Quantum radiating arrays and their directivity: A dynamical open system approach," *IEEE Antennas and Wireless Propagation Letters*, vol. 22, no. 3, pp. 536–540, 2023.

[51] R. Alaee, B. Gurlek, M. Albooyeh, *et al*., "Quantum metamaterials with magnetic response at optical frequencies," *Physical Review Letters*, vol. 125, no. 6, article no. 063601, 2020.

[52] I. Liberal and N. Engheta, "Nonradiating and radiating modes excited by quantum emitters in open epsilon-near-zero cavities," *Science Advances*, vol. 2, no. 10, article no. e1600987, 2016.

[53] H. J. Chang, S. H. Kim, Y. H. Lee, *et al*., "A photonic-crystal optical antenna for extremely large local-field enhancement," *Optics Express*, vol. 18, no. 23, pp. 24163–24177, 2010.

[54] S. Mikki and A. Kishk, "An efficient algorithm for the analysis and design of carbon nanotube photonic crystals," *Progress in Electromagnetics Research C*, vol. 83, pp. 83–96, 2018.

[55] S. Mikki, "Theory and computation of Markovian quantum antenna systems," *Results in Physics*, vol. 49, article no. 106453, 2023.

[56] Y. Chen, M. Zopf, R. Keil, *et al*., "Highly-efficient extraction of entangled photons from quantum dots using a broadband optical antenna," *Nature Communications*, vol. 9, no. 1, article no. 2994, 2018.

[57] F. Bello, N. Kongsuwan, J. F. Donegan, *et al*., "Controlled cavity-free, single-photon emission and bipartite entanglement of near-field-excited quantum emitters," *Nano Letters*, vol. 20, no. 8, pp. 5830–5836, 2020.

[58] A. Komarov and G. Slepyan, "Quantum antenna as an open system: Strong antenna coupling with photonic reservoir," *Applied Sciences*, vol. 8, no. 6, article no. 951, 2018.

[59] Y. V. Vladimirova and V. N. Zadkov, "Quantum optics of quantum emitters in the near field of a nanoparticle," *Physics-Uspekhi*, vol. 65, no. 3, article no. 245, 2022.

[60] G. S. Agarwal and D. Mukhopadhyay, "Coupling quantum antennas to fibers and waveguides," *arXiv preprint*, arXiv: 2111.03200, 2021.

[61] J. Z. Yang, C. Nawrath, R. Keil, *et al*., "Quantum dot-based broadband optical antenna for efficient extraction of single photons in the telecom O-band," *Optics Express*, vol. 28, no. 13, pp. 19457–19468, 2020.

[62] M. Casariego, E. Z. Cruzeiro, S. Gherardini, *et al*., "Propagating quantum microwaves: Towards applications in communication and sensing," *Quantum Science and Technology*, vol. 8, no. 2, article no. 023001, 2023.

[63] J. Klauder and E. C. G. Sudarshan, *Fundamentals of Quantum Optics*. Dover Publications, Mineola, NY, USA, 2006.

[64] V. Gorini, A. Kossakowski, and E. C. G. Sudarshan, "Completely positive dynamical semigroups of *N*-level systems," *Journal of Mathematical Physics*, vol. 17, no. 5, pp. 821–825, 1976.

[65] H. P. Breuer and F. Petruccione, *The Theory of Open Quantum Systems*. Oxford University Press, Oxford, UK, 2002.

[66] A. Rivas and S. F. Huelga, *Open Quantum Systems: An Introduction*. Springer, Berlin, Germany, 2011.

[67] M. H. Chang, *Quantum Stochastics*. Cambridge University Press, New York, NY, USA, 2015.

[68] S. Banerjee, *Open Quantum Systems: Dynamics of Nonclassical Evolution*. Springer, Singapore, 2018.

[69] S. Imre and F. Balázs, *Quantum Computing and Communications: An Engineering Approach*. Wiley, Hoboken, NJ, USA, 2005.

[70] M. Nielsen and I. L. Chuang, *Quantum Computation and Quantum Information*. Cambridge University Press, New York, NY, USA, 2010.

[71] J. G. van Bladel, *Electromagnetic Fields*. Wiley-Intersience, Hoboken, NJ, USA, 2007.

[72] Y. W. Zhang, A. Chen, W. Z. Liu, *et al*., "Observation of polarization vortices in momentum space," *Physical Review Letters*, vol. 120, no. 18, article no. 186103, 2018.

[73] S. Mikki, "Theory of electromagnetic radiation in nonlocal metamaterials—Part I: Foundations," *Progress in Electromagnetics Research B*, vol. 89, pp. 63–86, 2020.

[74] S. Mikki, "Theory of electromagnetic radiation in nonlocal metamaterials—Part II: Applications," *Progress in Electromagnetics Research B*, vol. 89, pp. 87–109, 2020.

[75] D. H. Lin, "Controlling matter waves in momentum space," *Physical Review A*, vol. 90, no. 1, article no. 012709, 2014.

[76] O. Keller, *Quantum Theory of Near-Field Electrodynamics*. Springer, Berlin, Germany, 2011.

[77] D. Kaiser, *Quantum Field Theory: Lectures of Sidney Coleman*. World Scientific, New Jersey, USA, 2019.

[78] L. Mandel and E. Wolf, *Optical Coherence and Quantum Optics*. Cambridge University Press, Cambridge, UK, 1995.

[79] M. O. Scully and M. S. Zubairy, *Quantum Optics*. Cambridge University Press, Cambridge, UK, 2012.

[80] R. J. Glauber, *Quantum Theory of Optical Coherence: Selected Papers and Lectures*. Wiley-VCH, Weinheim, Germany, 2007.

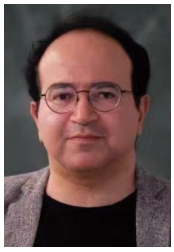
[81] S. Haroche and J. M. Raimond, *Exploring the Quantum: Atoms, Cavities and Photons*. Oxford University Press, Oxford, UK, 2006.

[82] T. D. Newton and E. P. Wigner, "Localized states for elementary systems," *Reviews of Modern Physics*, vol. 21, no. 3, pp. 400–406, 1949.

[83] W. O. Amrein, "Localizability for particles of mass zero," *Helvetica Physica Acta*, vol. 42, pp. 149–190, 1969.

[84] D. R. Grigore, "Uniqueness of the Newton-Wigner position operator," *International Journal of Theoretical Physics*, vol. 32, no. 4,

pp. 555–563, 1993.
[85] W. Heisenberg, *The Physical Principles of the Quantum Theory*. Dover Publications, New York, NY, USA, 1950.
[86] J. C. Garrison and R. Chiao, *Quantum Optics*. Oxford University Press, Oxford, UK, 2014.
[87] P. Coleman, *Introduction to Many-Body Physics*. Cambridge University Press, Cambridge, UK, 2015.
[88] W. Appel, *Mathematics for Physics and Physicists*. E. Kowalski, trans. Princeton University Press, Princeton, NJ, USA, 2007.
[89] S. Mikki, "Exact derivation of the radiation law of antennas embedded into generic nonlocal metamaterials: A momentum-space approach," in *Proceedings of the 14th European Conference on Antennas and Propagation (EuCAP)*, Copenhagen, Denmark, pp. 1–5, 2020.
[90] C. Roychoudhuri, A. F. Kracklauer, and K. Creath, *The Nature of Light: What is A Photon?*. CRC Press, Boca Raton, FL, USA, 2008.
[91] M. H. L. Pryce, "The mass-centre in the restricted theory of relativity and its connexion with the quantum theory of elementary particles," *Proceedings of the Royal Society A: Mathematical, Physical and Engineering Sciences*, vol. 195, no. 1040, pp. 62–81, 1948.
[92] A. S. Wightman, "On the localizability of quantum mechanical systems," *Reviews of Modern Physics*, vol. 34, no. 4, pp. 845–872, 1962.
[93] T. O. Philips, "Lorentz invariant localized states," *Physical Review*, vol. 136, no. 3B, pp. B893–B896, 1964.
[94] J. E. M. Ingall, "The Newton-Wigner and Wightman localization of the photon," *Foundations of Physics*, vol. 26, no. 8, pp. 1003–1031, 1996.
[95] M. Hawton and V. Debierre, "Maxwell meets Reeh-Schlieder: The quantum mechanics of neutral bosons," *Physics Letters A*, vol. 381, no. 23, pp. 1926–1935, 2017.
[96] R. Haag, *Local Quantum Physics: Fields, Particles, Algebras*. Springer-Verlag, New York, NY, USA, 1992.
[97] M. Hawton and W. E. Baylis, "Photon position operators and localized bases," *Physical Review A*, vol. 64, no. 1, article no. 012101, 2001.
[98] P. Teller, *An Interpretive Introduction to Quantum Field Theory*. Princeton University Press, Princeton, NJ, USA, 1997.
[99] I. Ojima and H. Saigo, "Photon localization revisited," *Mathematics*, vol. 3, no. 3, pp. 897–912, 2015.
[100] I. H. Deutsch and J. C. Garrison, "Paraxial quantum propagation," *Physical Review A*, vol. 43, no. 5, pp. 2498–2513, 1991.
[101] E. M. Henley and W. Thirring, *Elementary Quantum Field Theory*. McGraw-Hill, New York, NY, USA, 1962.
[102] L. Mandel, "Configuration-space photon number operators in quantum optics," *Physical Review*, vol. 144, no. 4, pp. 1071–1077, 1966.
[103] W. Greiner and J. Reinhardt, *Field Quantization*. Springer, Berlin, Germany, 1996.
[104] V. B. Berestetskii, E. M. Lifshitz, and L. P. Pitaevskii, *Quantum Electrodynamics*, 2nd ed., Pergamon Press, Oxford, UK, 1982.
[105] I. H. Deutsch, "A basis-independent approach to quantum optics," *American Journal of Physics*, vol. 59, no. 9, pp. 834–839, 1991.
[106] P. W. Milonni, *An Introduction to Quantum Optics and Quantum Fluctuations*. Oxford University Press, Oxford, UK, 2019.
[107] G. Lindblad, "On the generators of quantum dynamical semigroups," *Communications in Mathematical Physics*, vol. 48, no. 2, pp. 119–130, 1976.
[108] M. Riesch and C. Jirauschek, "Analyzing the positivity preservation of numerical methods for the Liouville-von Neumann equation," *Journal of Computational Physics*, vol. 390, pp. 290–296, 2019.
[109] C. H. Wilcox, "An expansion theorem for electromagnetic fields," *Communications on Pure and Applied Mathematics*, vol. 9, no. 2, pp. 115–134, 1956.
[110] C. Cohen-Tannoudji, J. Dupont-Roc, and G. Grynberg, *Photons and Atoms: Introduction to Quantum Electrodynamics*. Wiley, New York, NY, USA, 1989.
[111] J. D. Jackson, *Classical Electrodynamics*, 3rd ed., Wiley, New York, NY, USA, 1999.
[112] P. W. Milonni, *Fast Light, Slow Light and Left-Handed Light*. Institute of Physics, Bristol, PA, USA, 2005.
[113] P. M. Morse and H. Feshbach, *Methods of Theoretical Physics*. McGraw Hill, New York, NY, USA, 1953.
[114] E. C. G. Sudarshan, "Equivalence of semiclassical and quantum mechanical descriptions of statistical light beams," *Physical Review Letters*, vol. 10, no. 7, pp. 277–279, 1963.
[115] R. A. Horn and C. R. Johnson, *Matrix Analysis*, 2nd ed., Cambridge University Press, Cambridge, UK, 2012.
[116] S. Mikki, S. Clauzier, and Y. Antar, "A correlation theory of antenna directivity with applications to superdirective arrays," *IEEE Antennas and Wireless Propagation Letters*, vol. 18, no. 5, pp. 811–815, 2019.
[117] R. H. Shi, J. J. Shi, Y. Guo, *et al*., "Quantum MIMO communication scheme based on quantum teleportation with triplet states," *International Journal of Theoretical Physics*, vol. 50, no. 8, pp. 2334–2346, 2011.
[118] J. Park, Y. Seo, and J. Heo, "Applications of a quantum linear system algorithm to linear MIMO detections," *IEEE Access*, vol. 10, pp. 36233–36245, 2022.
[119] M. M. Wilde, *Quantum Information Theory*, 2nd ed., Cambridge University Press, Cambridge, UK, 2017.
[120] G. Cariolaro, *Quantum Communications*. Springer, Cham, Germany, 2016.
[121] W. H. Louisell, *Radiation and Noise in Quantum Electronics*. R. E. Krieger Pub. Co., Huntington, NY, USA, 1977.
[122] H. A. Bachor and T. C. Ralph, *A Guide to Experiments in Quantum Optics*, 3rd ed., Blackwell Verlag, Weinheim, Germany, 2019.
[123] Z. J. Ou, *Quantum Optics for Experimentalists*. World Scientific Publishing, Singapore, 2017.
[124] L. Mandel, E. C. G. Sudarshan, and E. Wolf, "Theory of photoelectric detection of light fluctuations," *Proceedings of the Physical Society*, vol. 84, no. 3, pp. 435–444, 1964.



Said Mikki received the Ph.D. degree in electrical engineering from University of Mississippi, Oxford, MS, USA, in 2008. He is currently an Associate Professor in electrical engineering with the Zhejiang University-University of Illinois at Urbana-Champaign (ZJU-UIUC) Institute, Zhejiang University, Haining, China, and the Department of Electrical and Computer Engineering, University of Illinois at Urbana-Champaign, Urbana, IL, USA. His current research interests include quantum engineering, electromagnetics, information theory, and artificial intelligence.
(Email: smikki@illinois.edu)